



**The Abdus Salam
International Centre for Theoretical Physics**



1965-26

**9th Workshop on Three-Dimensional Modelling of Seismic Waves
Generation, Propagation and their Inversion**

22 September - 4 October, 2008

Upper Mantle Anisotropy from Surface Wave Studies

Part I

Jean-Paul Montagner

Dept. Sismologie

I.P.G.

Paris

France



SURFACE WAVES and UPPER MANTLE ANISOTROPY



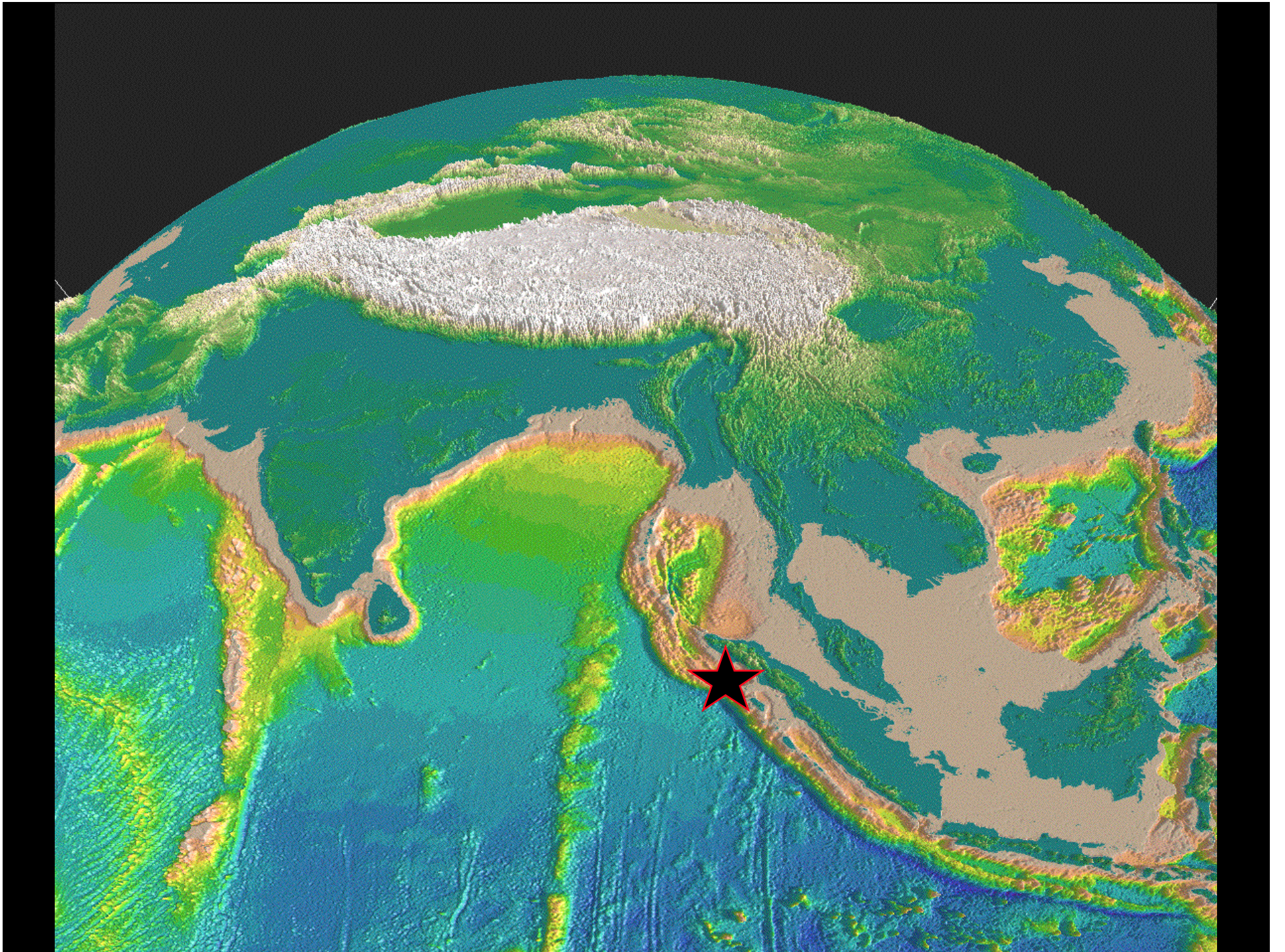
Jean-Paul Montagner

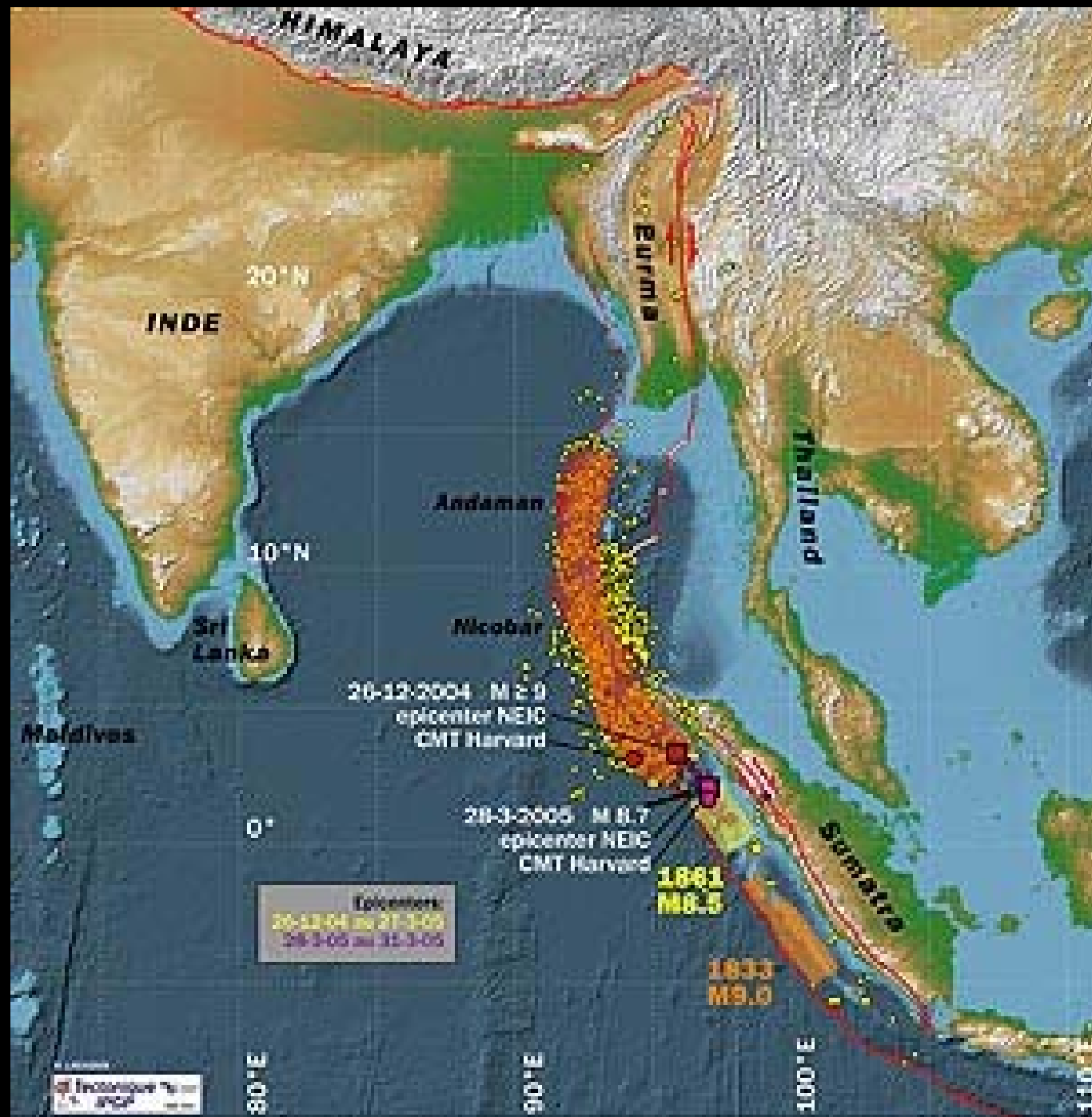
Dept. Sismologie, I.P.G., Paris; France

Overview

Large scale Seismology: an observational field

- Data (Seismic source) + Instrument (Seismometer) -> Observations (seismograms)
- Historical evolution: Ray theory, Normal mode theory, Numerical techniques (SEM, NM-SEM)
- Scientific Issues: Earthquakes (Sumatra-Andaman), Anisotropic structure of the Earth
- Tomographic Technique
- Geodynamic Applications
- Seismic Experiment: Plume detection
- Adjoint and time reversal methods



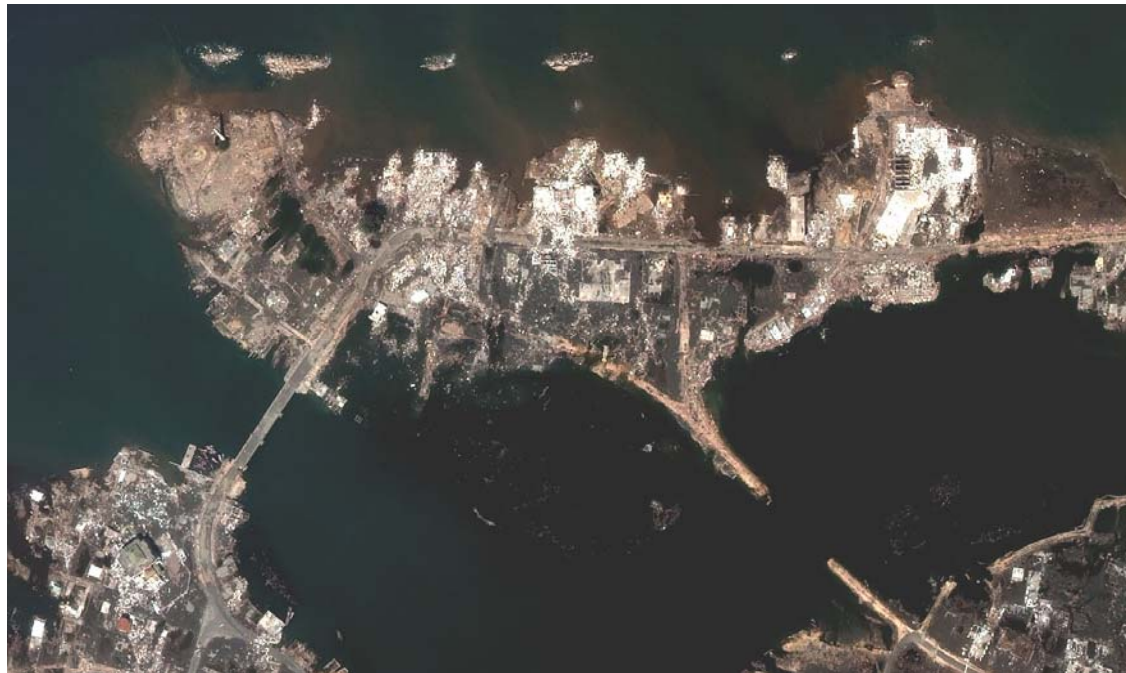


Banda Aceh

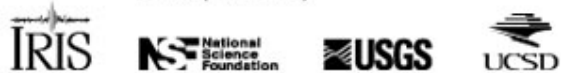
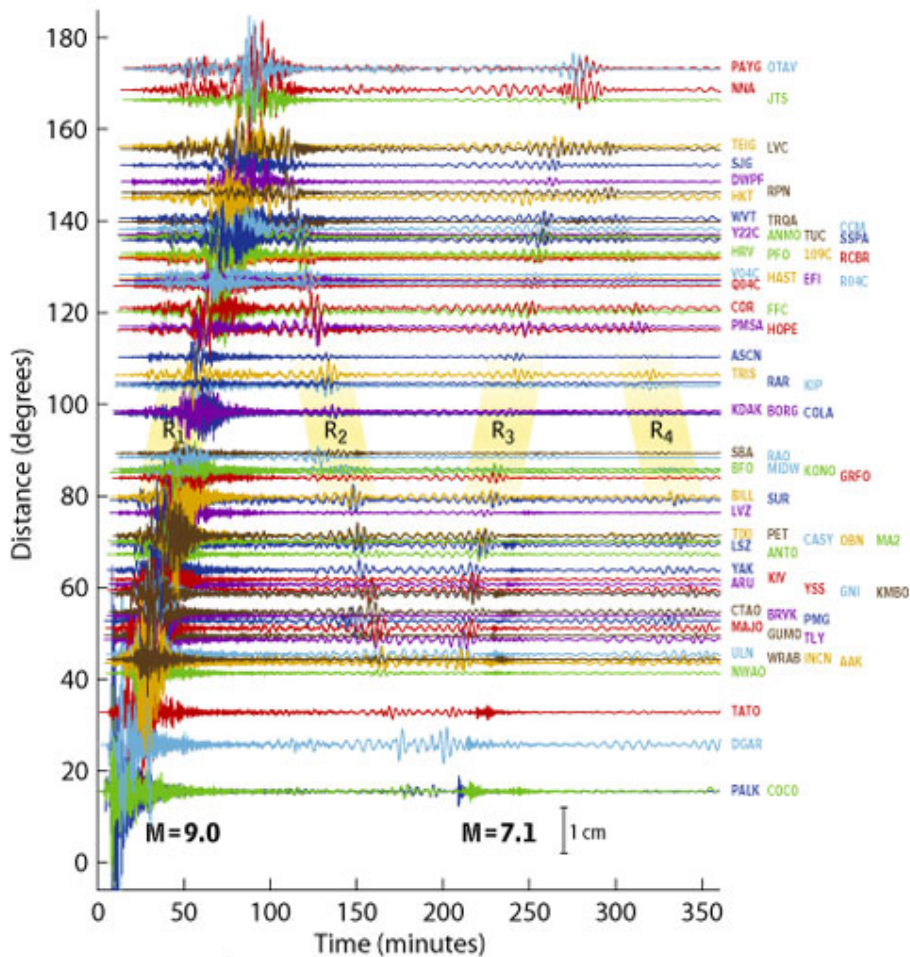
before



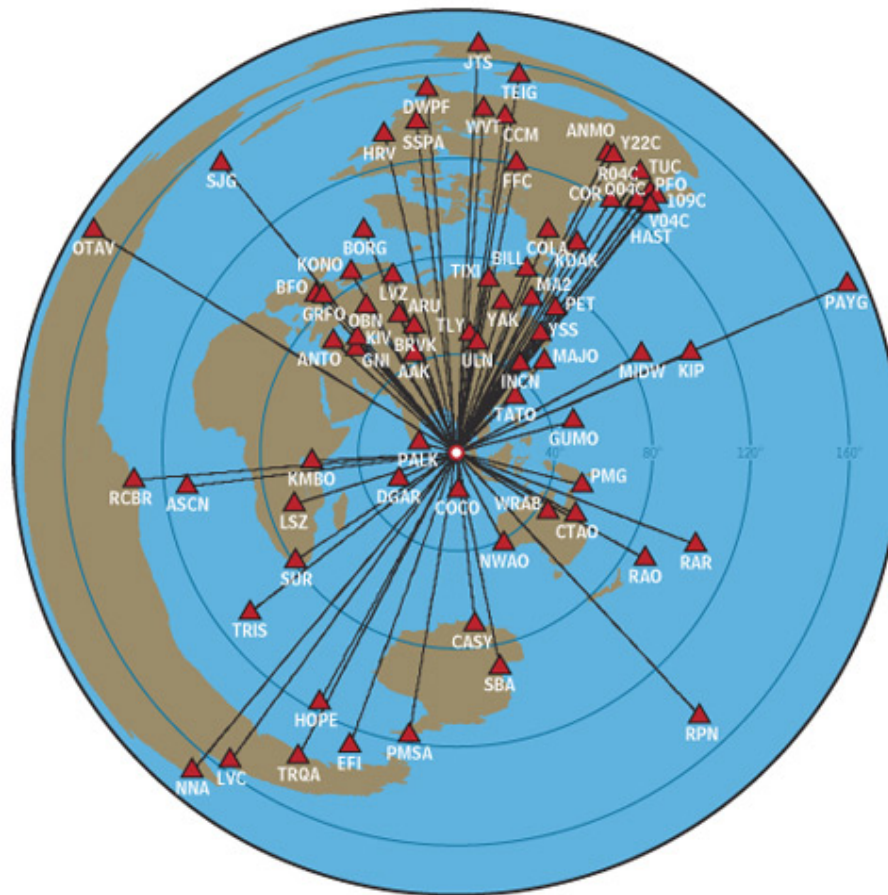
after



Sumatra - Andaman Islands Earthquake ($M_w=9.0$)
Global Displacement Wavefield from the Global Seismographic Network



Sumatra - Andaman Islands Earthquake
Global Seismographic Network Stations

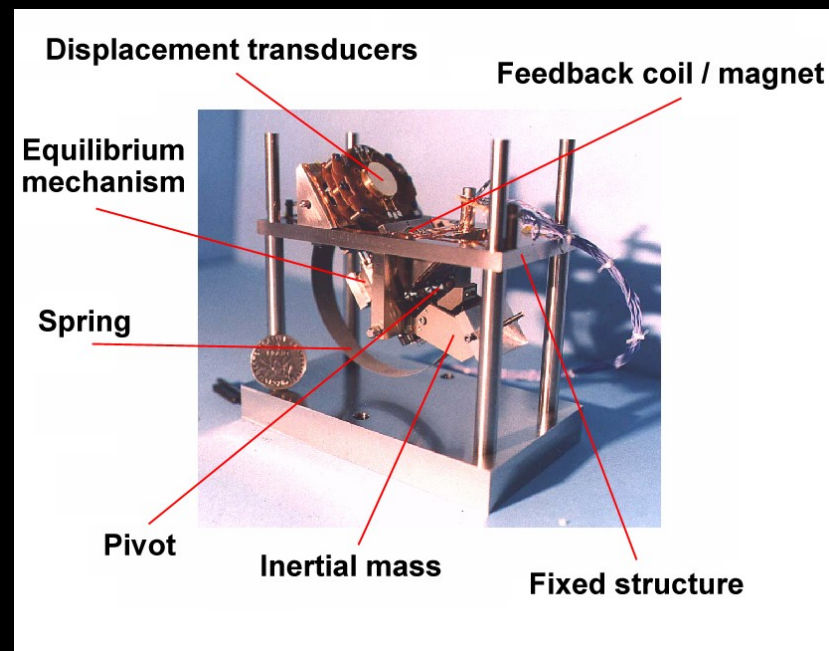


Seismic Instruments

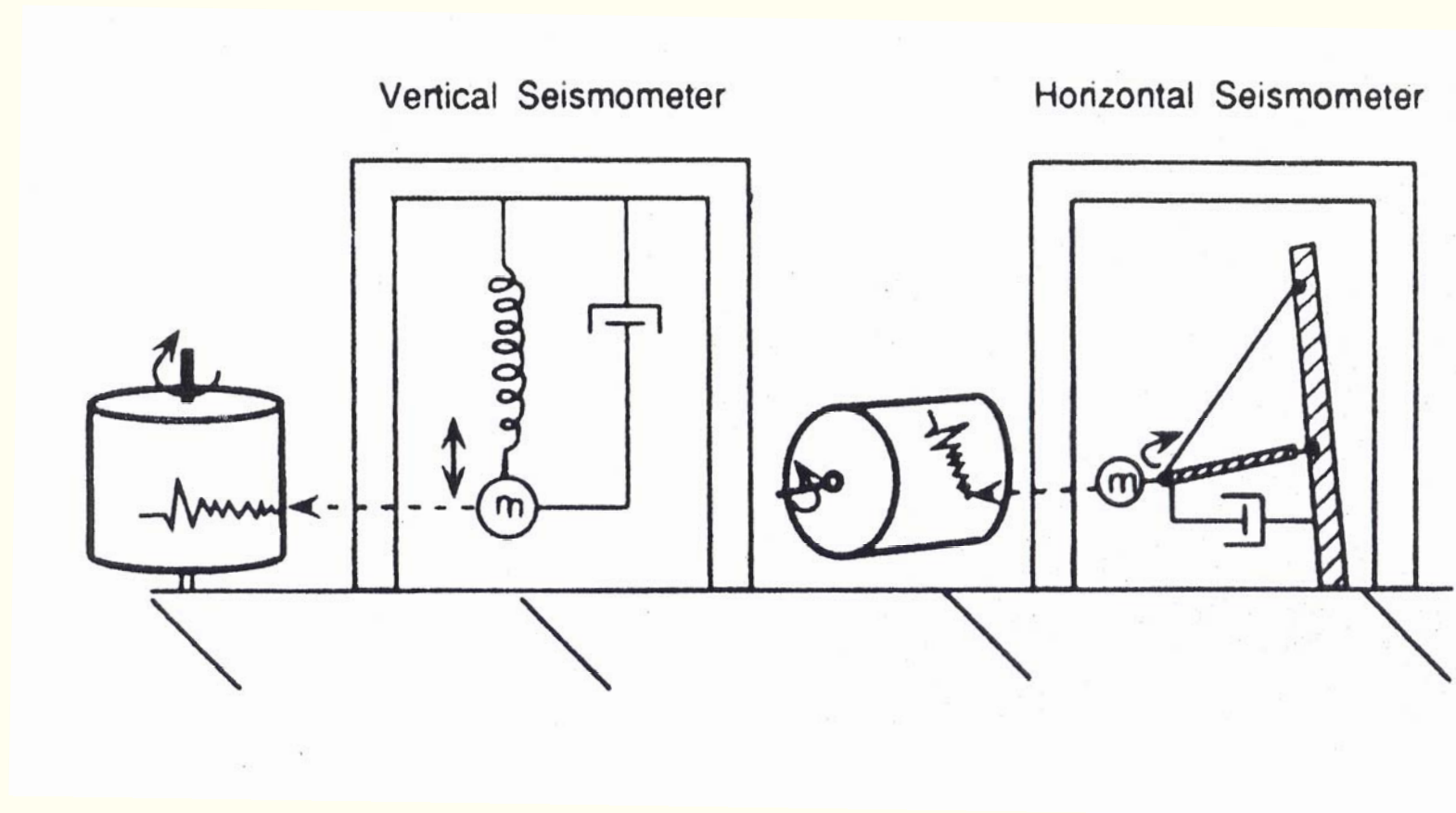
- Seismoscope
(China -100BC)



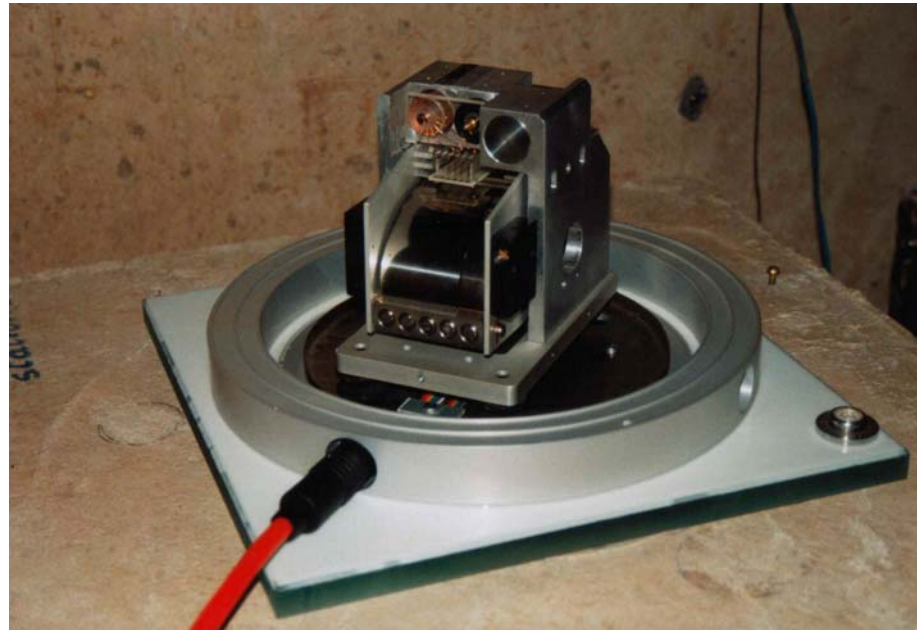
Broadband
Seismometer
(1mHz-20Hz)
(Cacho, 1998)



Principle of a Seismometer

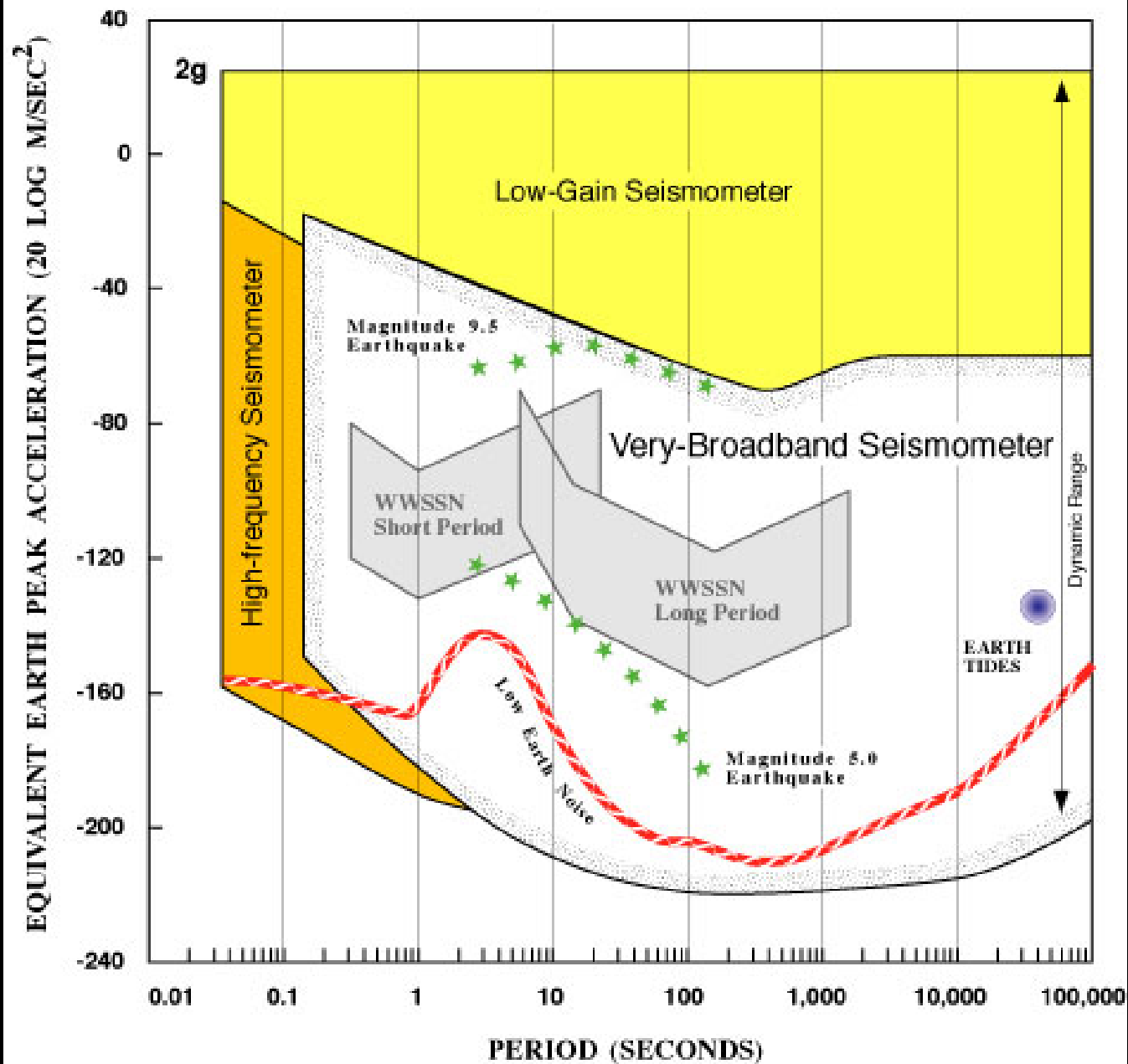


Tiltmeter (1960)



Broadband Seismometer (1982)
Streckeisen STS1: $0.05\text{s} < T < 5000\text{s}$

IRIS GSN SYSTEM

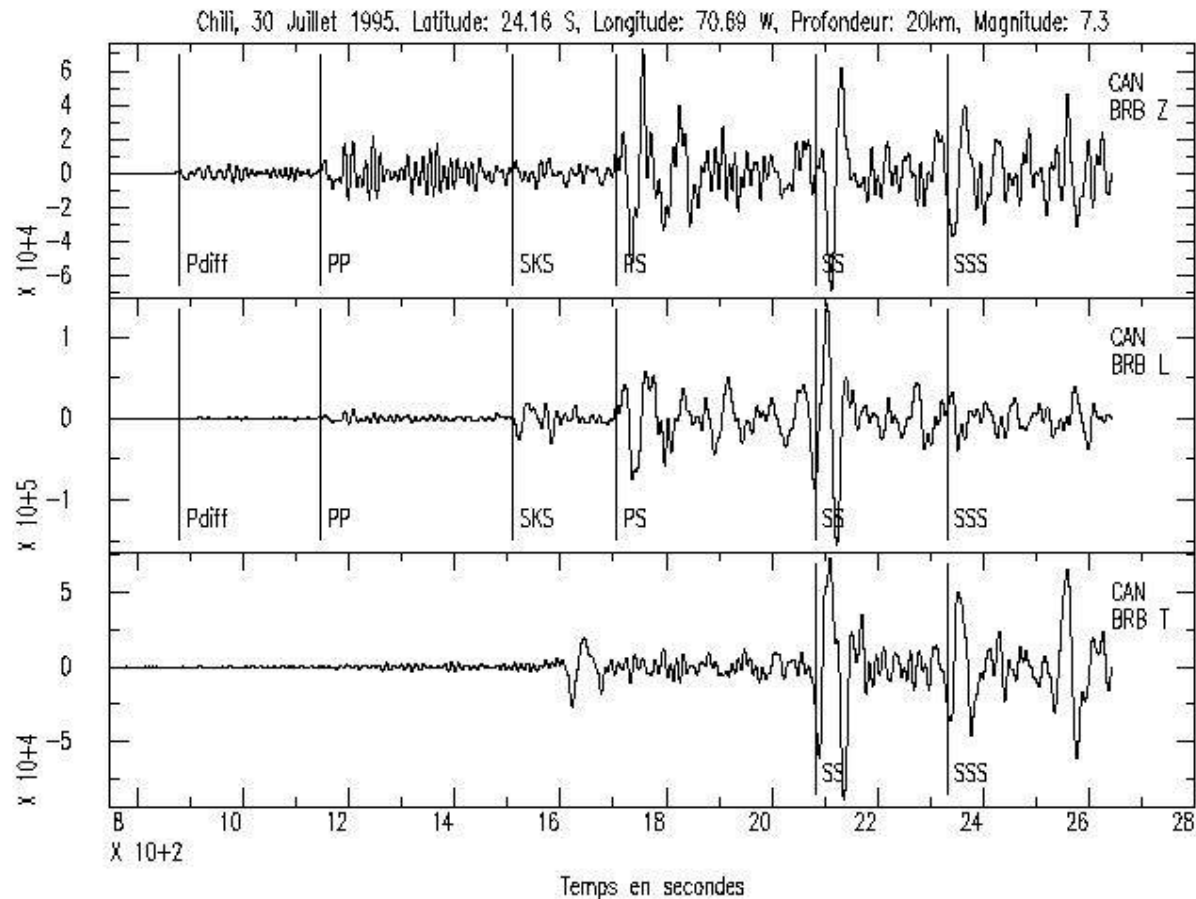


Butler et al., 2004

3 components

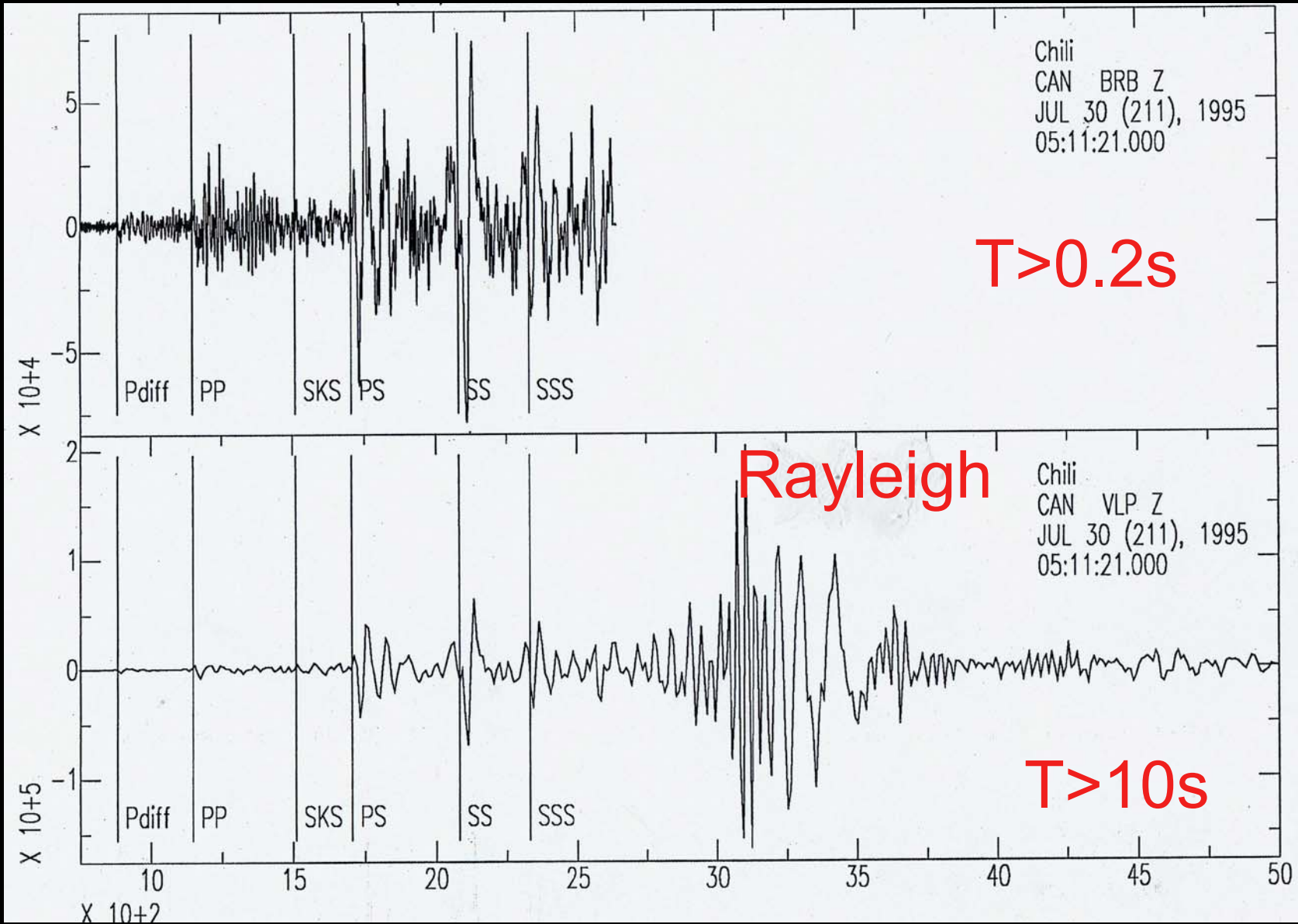
frequency range: 1mHz-20Hz
Period range: 0.05-1000s

Chile July 30, 1995, Ms=7.3

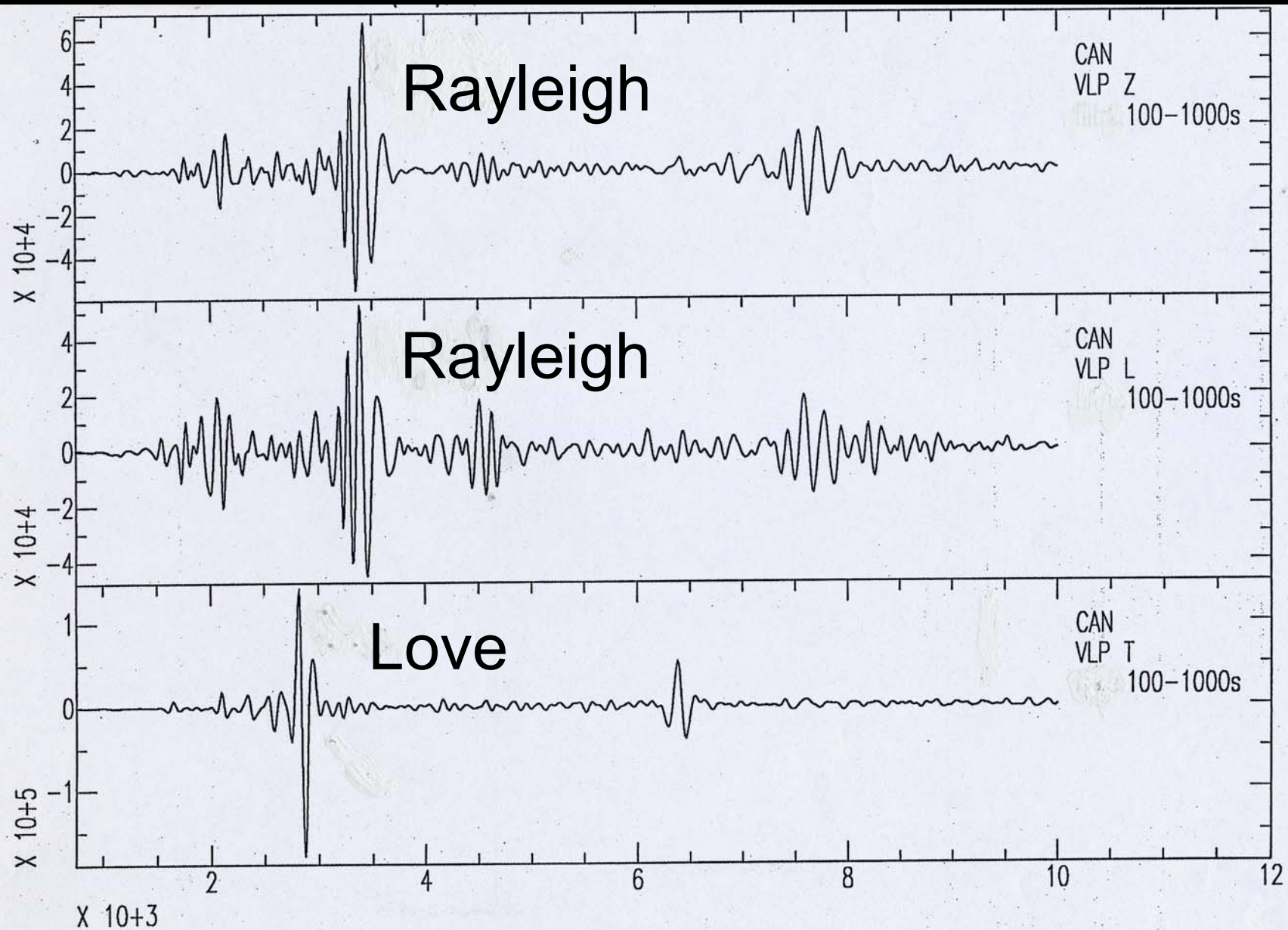


Chile earthquake magnitude= 7.3

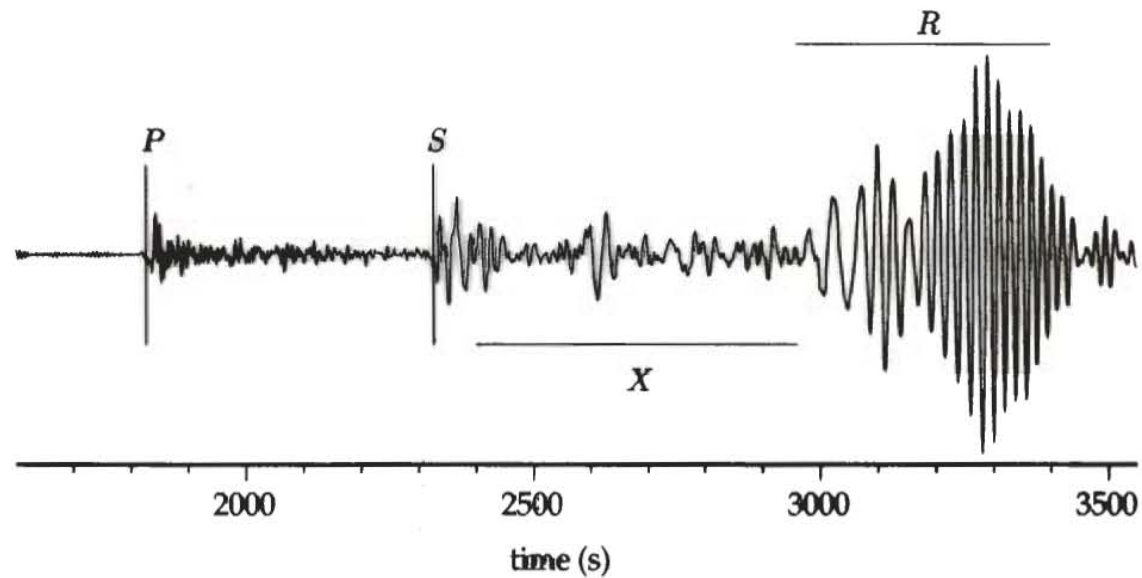
Epicentral distance = 12,300km-depth 20km



Chile Earthquake Jul. 1995

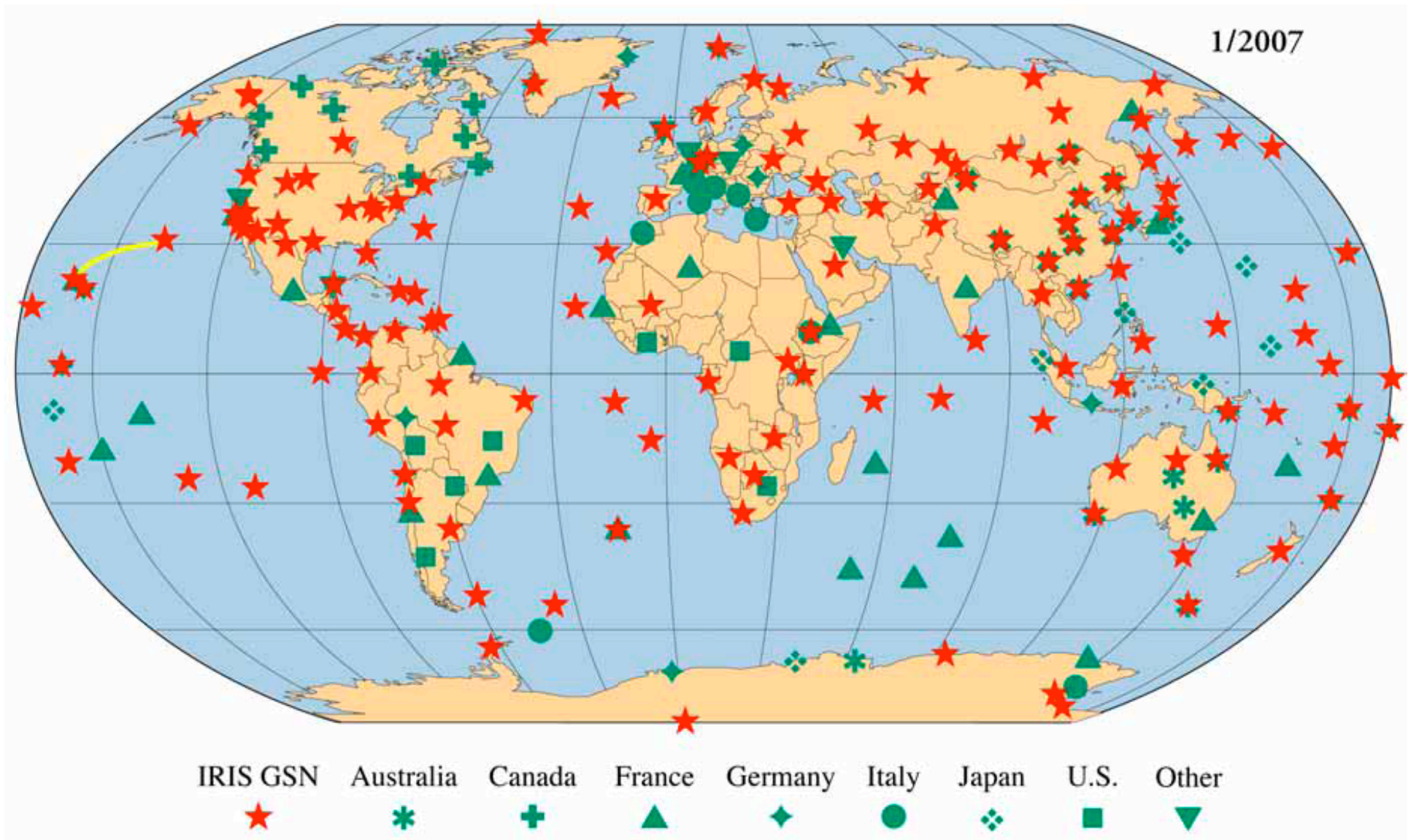


- Dispersive waves,
- Good global coverage,
- Large scale heterogeneities (min. 600 km).



Vertical component of displacement field recorded at DRV station corresponding to the New-Guinea 05/16/1999 earthquake.

F.D.S.N. (Federation of Digital Broadband Seismic Networks)

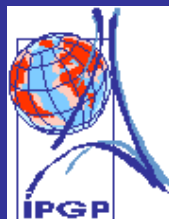


Ocean Bottom Observatories

=> International Ocean network
(I.O.N.)

- 2/3 of the Earth are covered by water.
- seafloor seismometers enable:
 - To investigate oceanic regions with a better resolution
 - To fill gaps in the global coverage

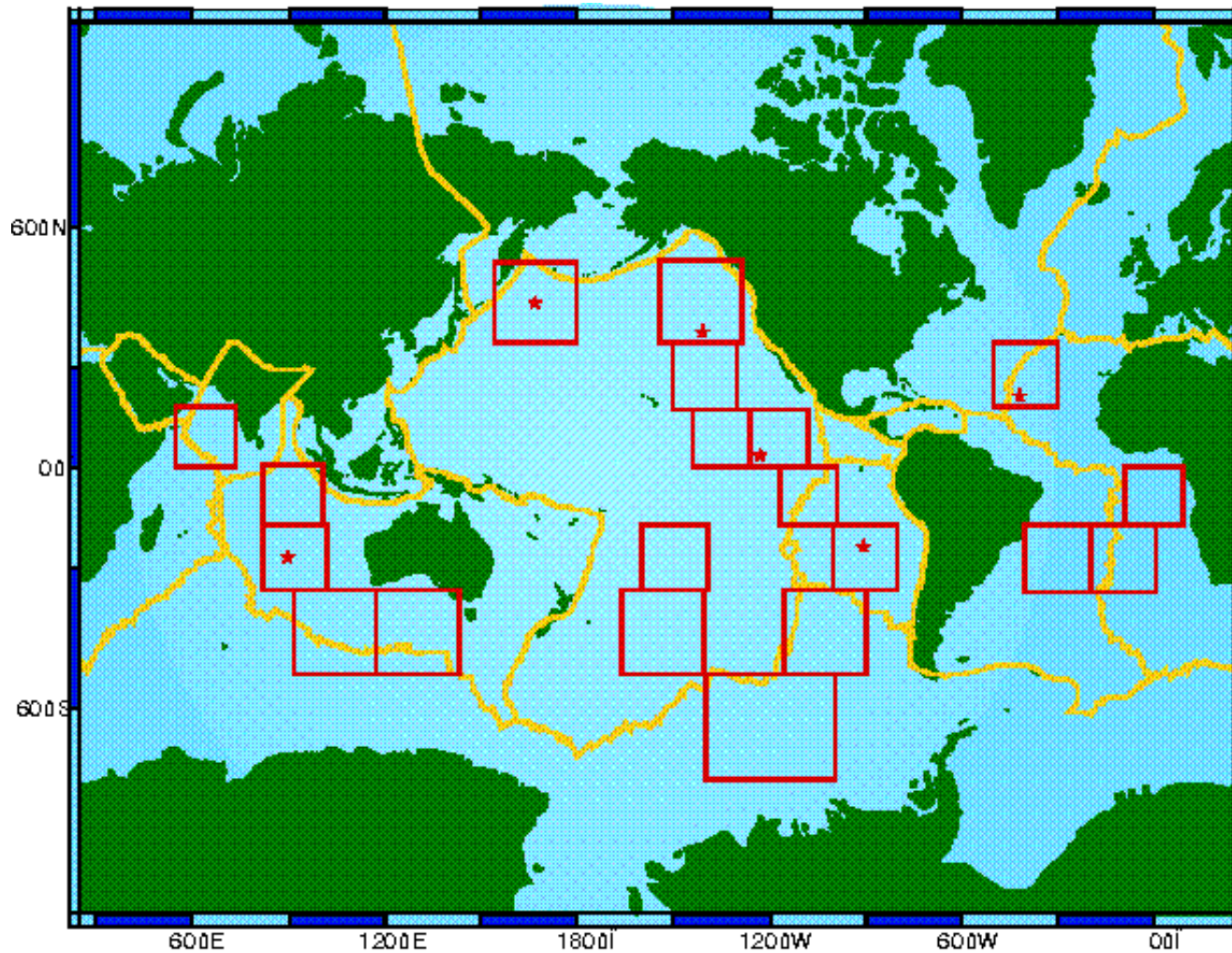
NERO (joint French-Japanese Project)



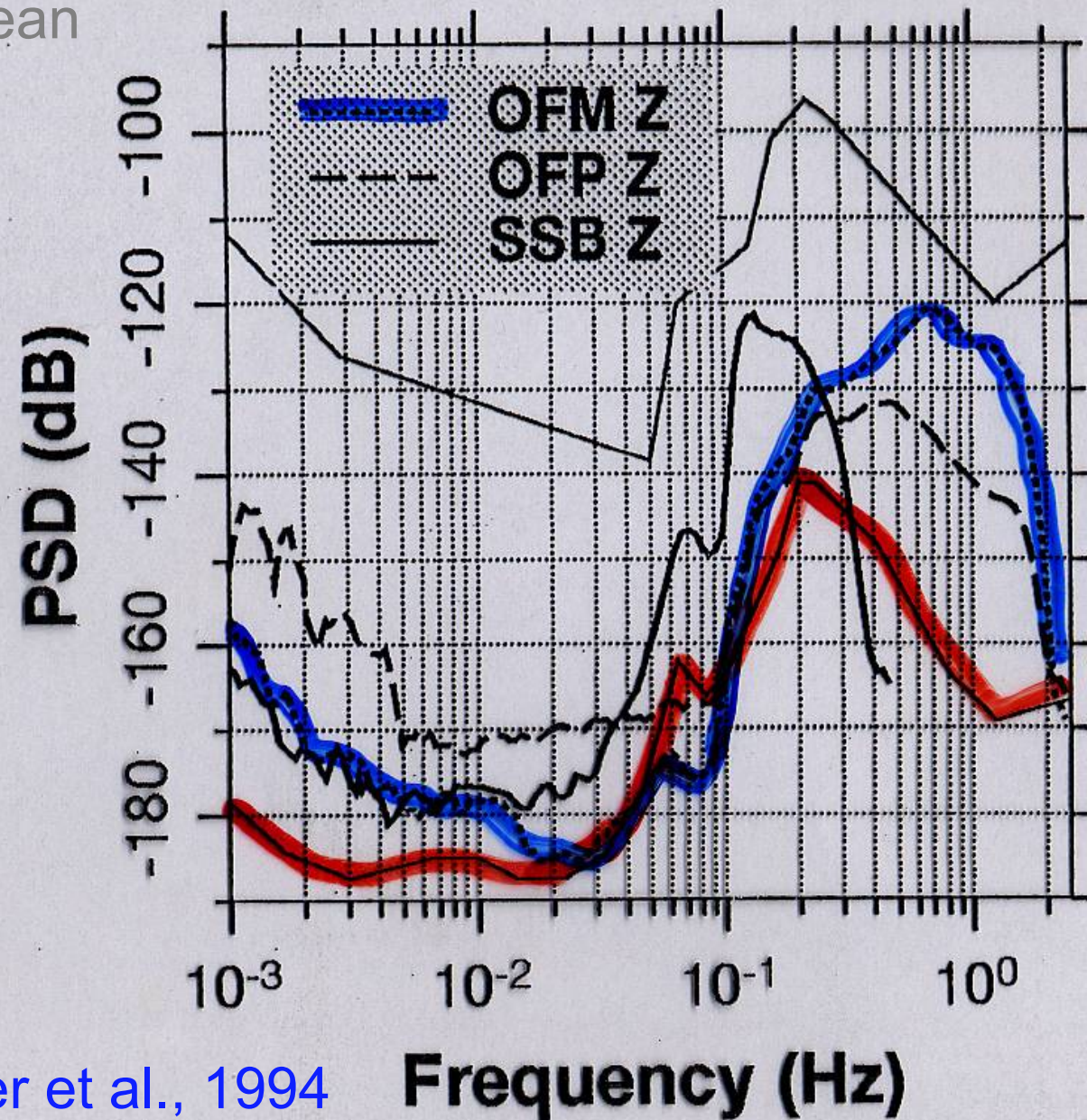
I.O.N.

International Ocean Network

ION (International Ocean network) France, Italy, Japan, UK, U.S.



OFM: Ocean
bottom
station



Montagner et al., 1994



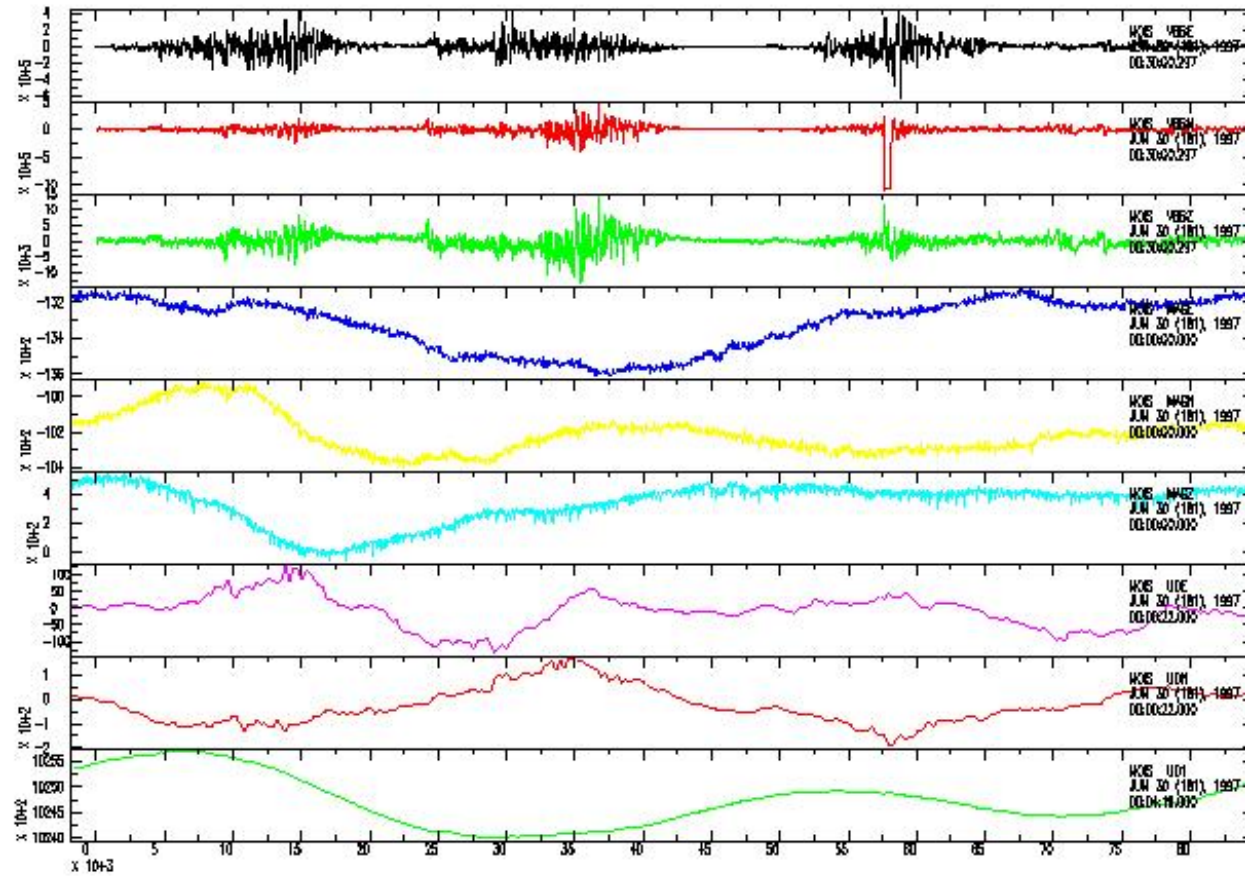
M.O.I.S.E (June-Sept. 1997)

(Monterey bay Ocean bottom International Experiment)

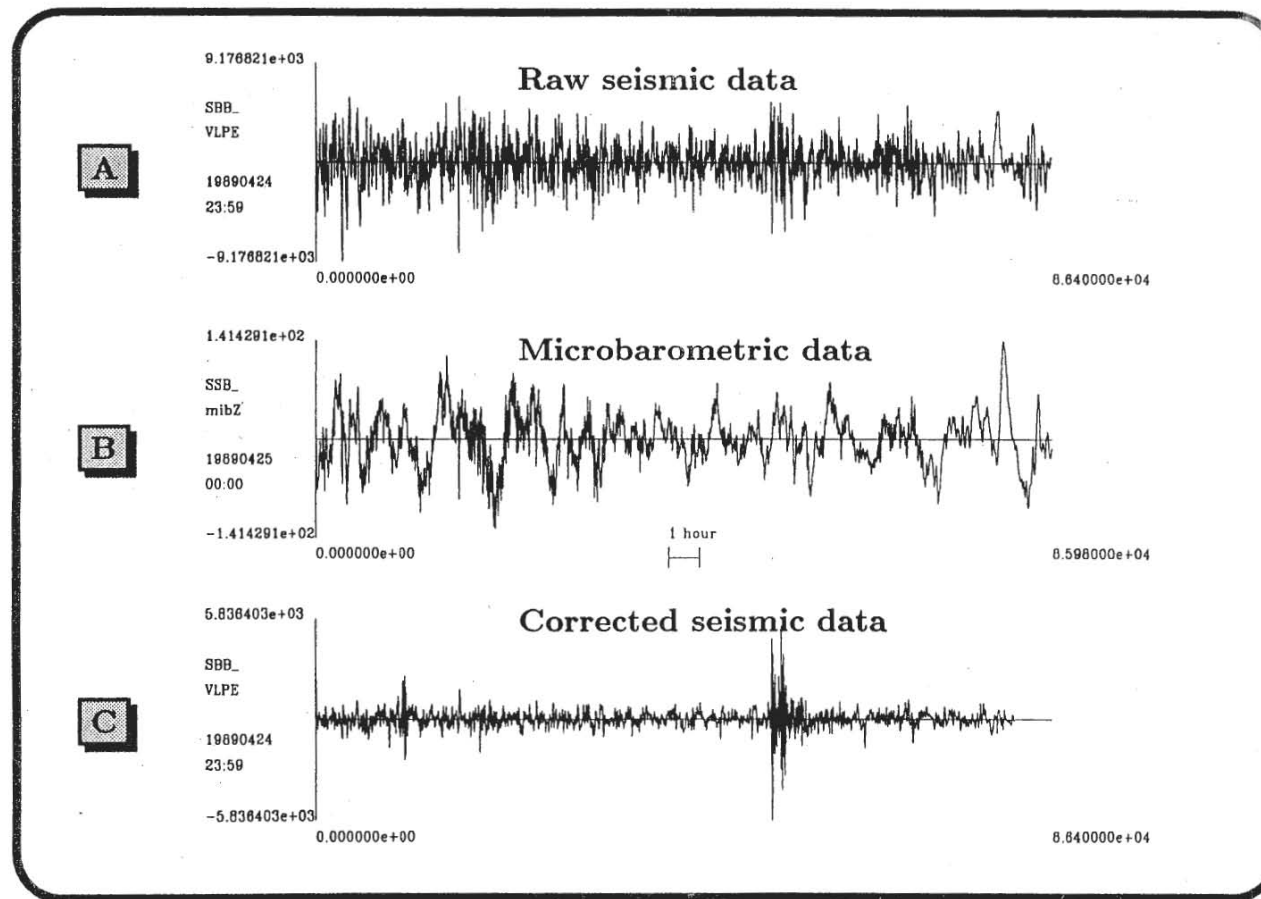
MBARI, UC Berkeley, IPG-Paris, UBO-Brest



Multiparameter signals



Deconvolution of the seismic signal from the pressure influence

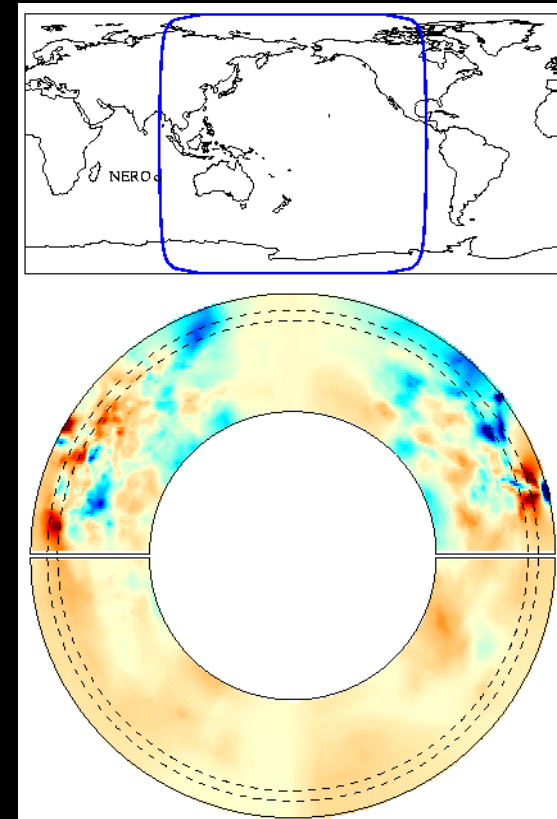




NERO observatory
Scientific Interest
Global scale

- To fill a gap in global station coverage
- To improve global tomographic model resolution
- To improve azimuthal distribution in determination of large earthquakes focal

NERO



Karason & van der Hilst, 2003

Project Seafloor Portable Seismometers



Crawford et al., 2002

Overview

Large scale Seismology: an observational field

- Data (Seismic source) + Instrument (Seismometer) -> Observations (seismograms)
- **Historical evolution: Ray theory, Normal mode theory, Numerical techniques (SEM, NM-SEM)**
- Scientific Issues: Earthquakes (Sumatra-Andaman), Anisotropic structure of the Earth
- Tomographic Technique
- Geodynamic Applications
Seismic Experiment, Plume detection
- Adjoint and time reversal methods

Propagation of seismic waves

Hypothesis: Elastic Medium : $\sigma_{ij} = C_{ijkl} \varepsilon_{kl}$

Where ε_{kl} is the strain tensor, σ_{ij} the stress tensor

C_{ijkl} the elastic tensor: 81 elastic moduli

Symmetries of ε_{kl} , σ_{ij} and of the strain energy

$W = 1/2 \sigma_{ij} \varepsilon_{ij} \Rightarrow 21$ independent elements

Isotropic case $\Rightarrow 2$ independent elements

$$C_{ijkl} = \lambda \delta_{ij} \delta_{kl} + \mu (\delta_{ik} \delta_{jl} + \delta_{il} \delta_{jk})$$

λ , μ are Lamé parameters

Elastodynamic equation of motion

$$\partial_j (C_{ijkl} \partial_k u_l) - \rho \partial_{tt} u_i = 0$$

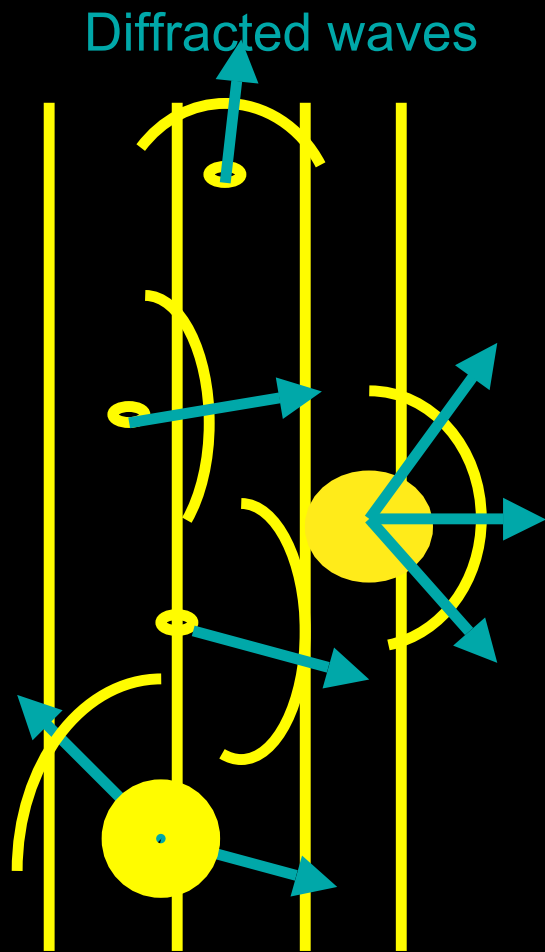
In the isotropic case, 2 solutions:

S-wave

P wave

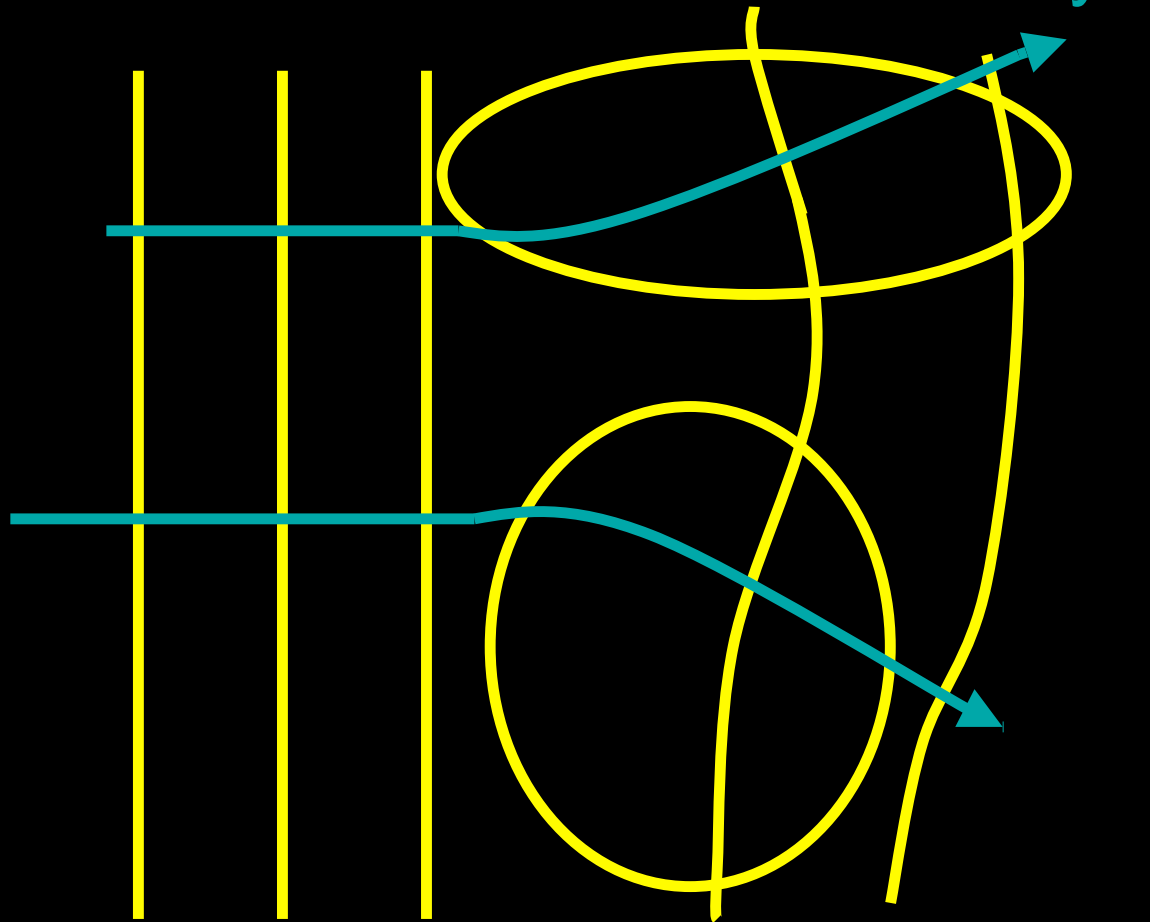
In heterogeneous media, comparison between
Wavelength λ and scale of heterogeneity Λ

Λ heterogeneity scale, λ wavelength



wavefronts

$\lambda \sim \Lambda$ or $\lambda \gg \Lambda$



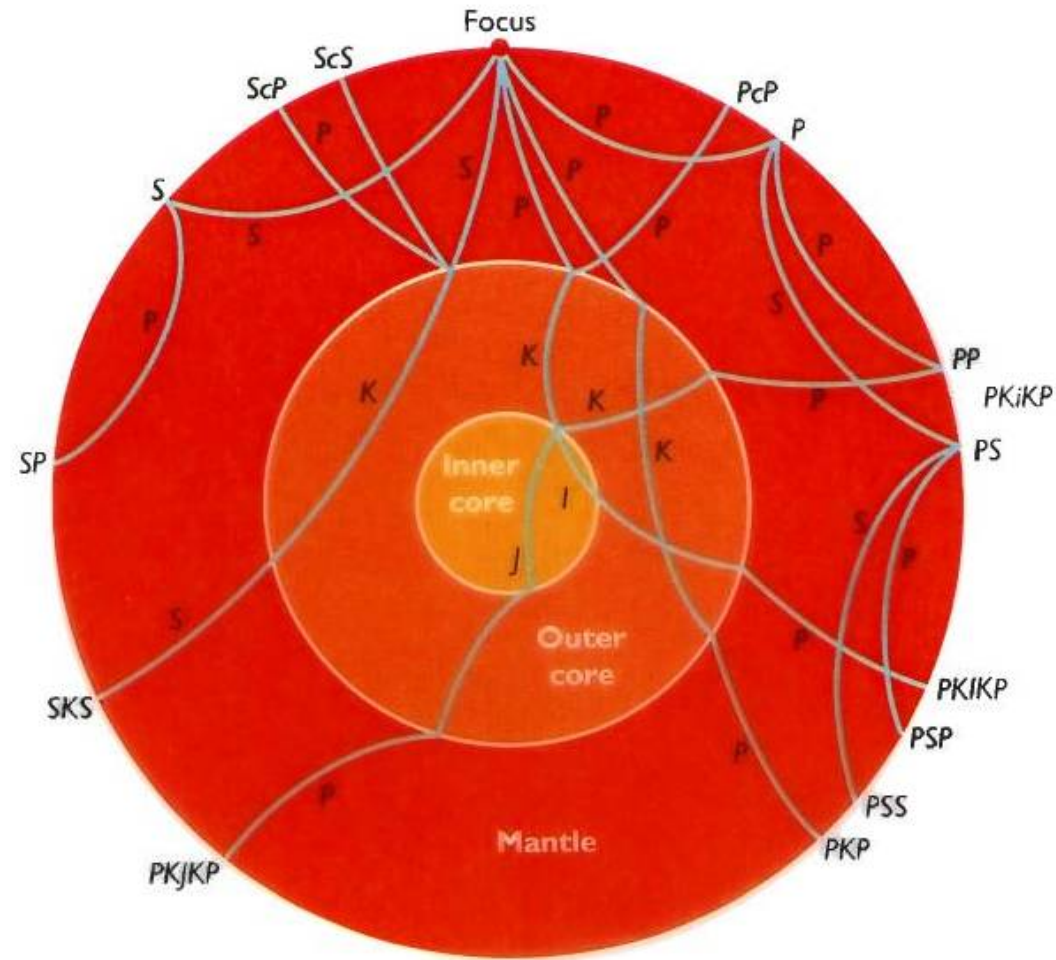
wavefronts

$\lambda \ll \Lambda$

Duality wave - particle:

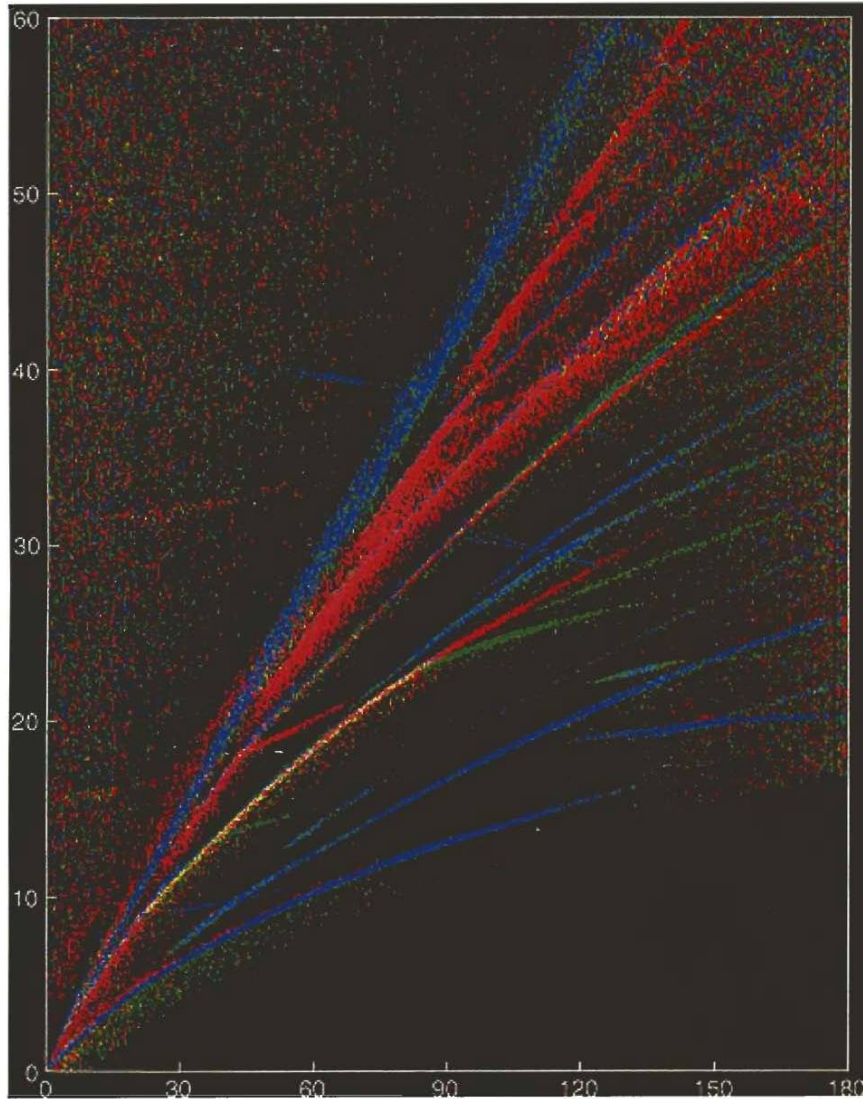
- λ seismic wavelength
- Λ scale heterogeneity
- Particle: Ray theory (XXth century)
 $\lambda \ll \Lambda$
- Wave: Normal mode theory (>1970)

RAY PATHS INSIDE THE EARTH



Bolt, 1993

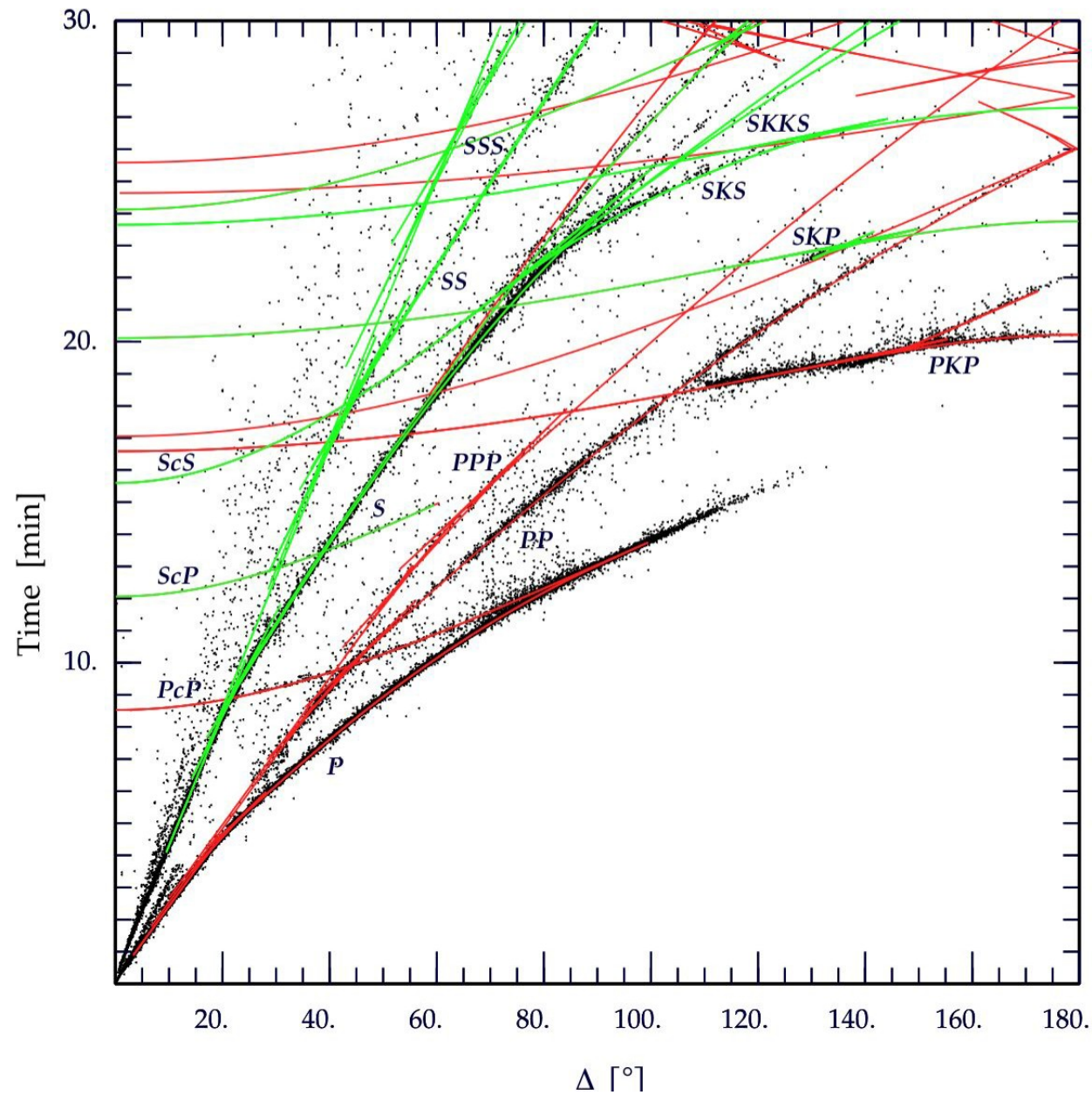
Time



Epicentral distance

Shearer, 1997

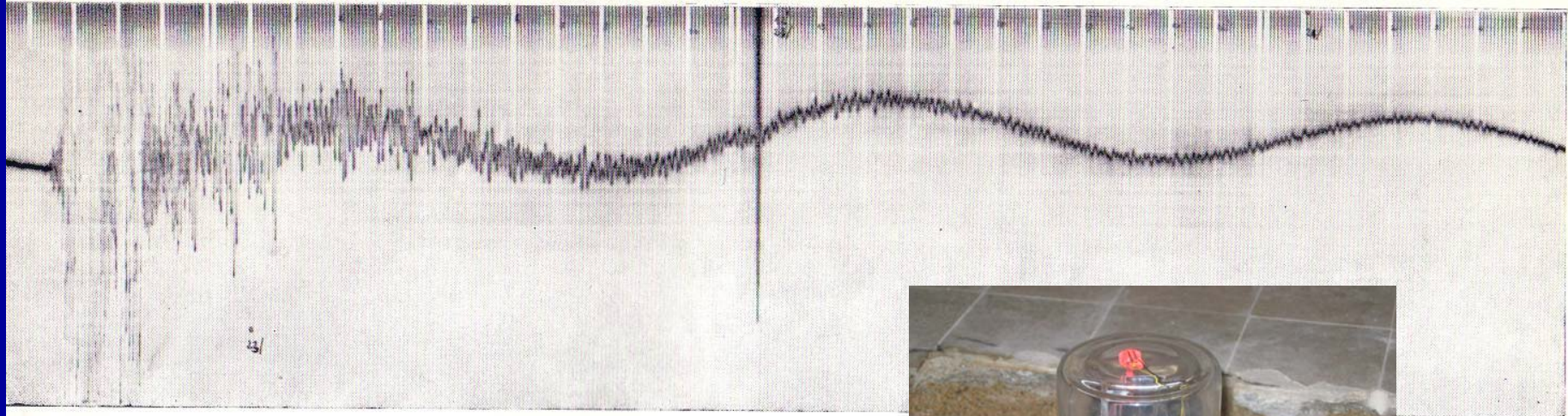
“Travel time” of certain seismic phases vs. epicentral distance



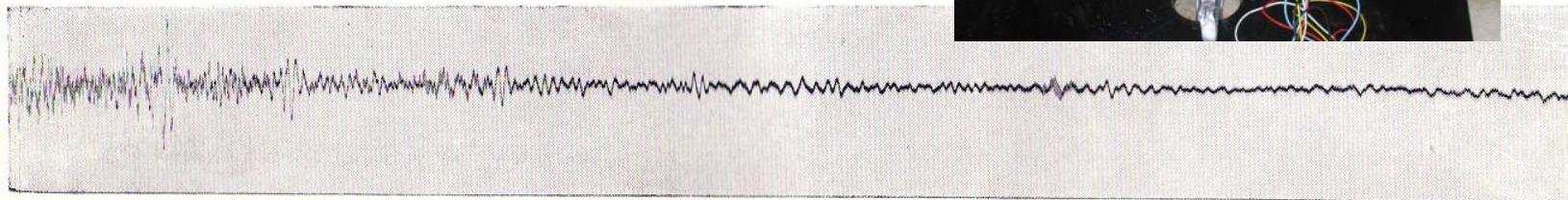
Duality wave - particle:

- λ seismic wavelength
- Λ scale heterogeneity
- Particle: Ray theory (XXth century)
 $\lambda \ll \Lambda$
- Wave: Normal mode theory (>1970)

Chile Earthquake (22 may 1960) recorded at Paris (IPGP)



1a



1b

FIG. 1. — a) Enregistrement du pendule E, n° 1 (voir tableau I).
b) Enregistrement du pendule B, n° 4 (voir tableau I). (Un intervalle de 5 minutes est représenté sur cette figure par 1,45 mm.)

Chile earthquake (may 22 1960) recorded at Paris (IPGP)

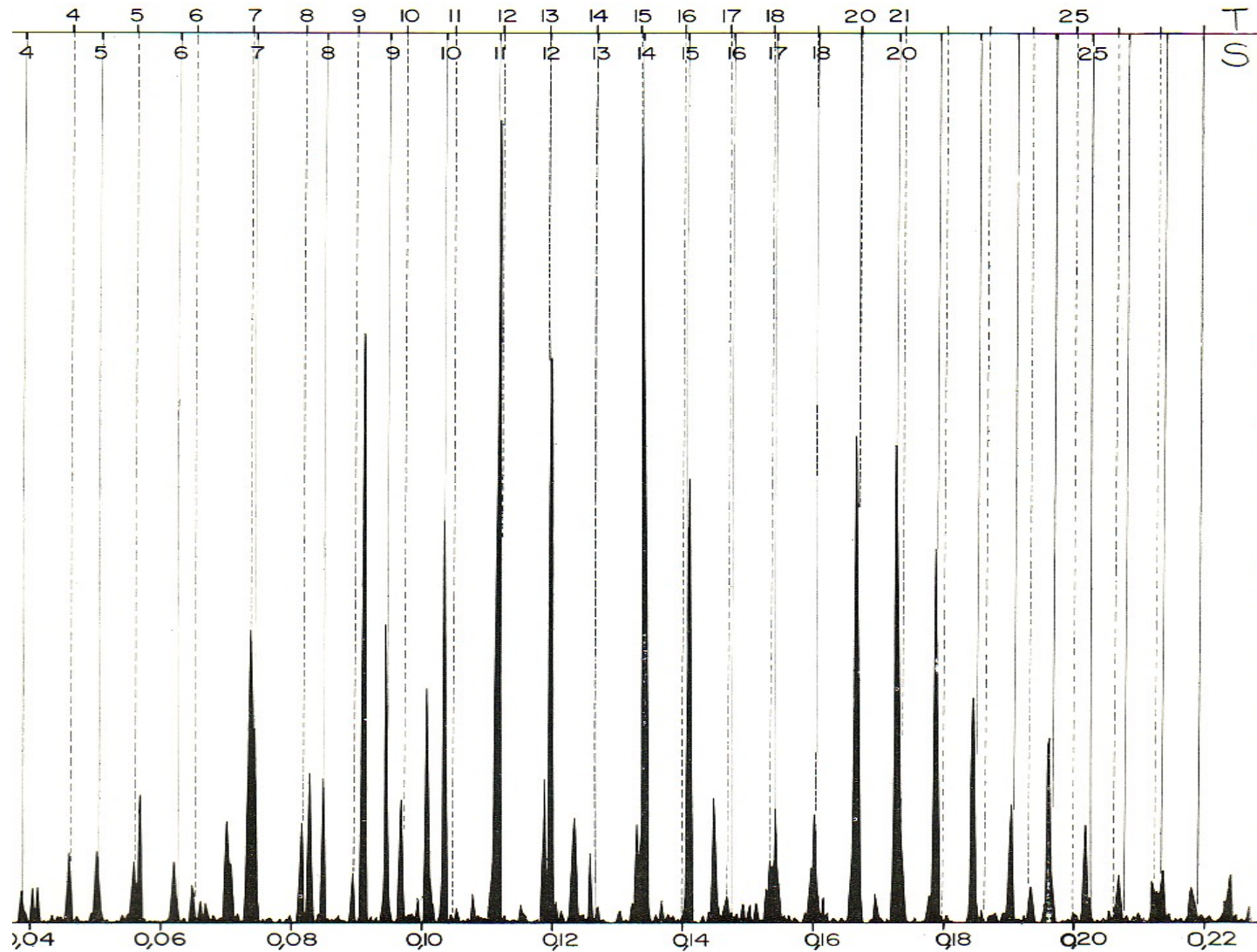


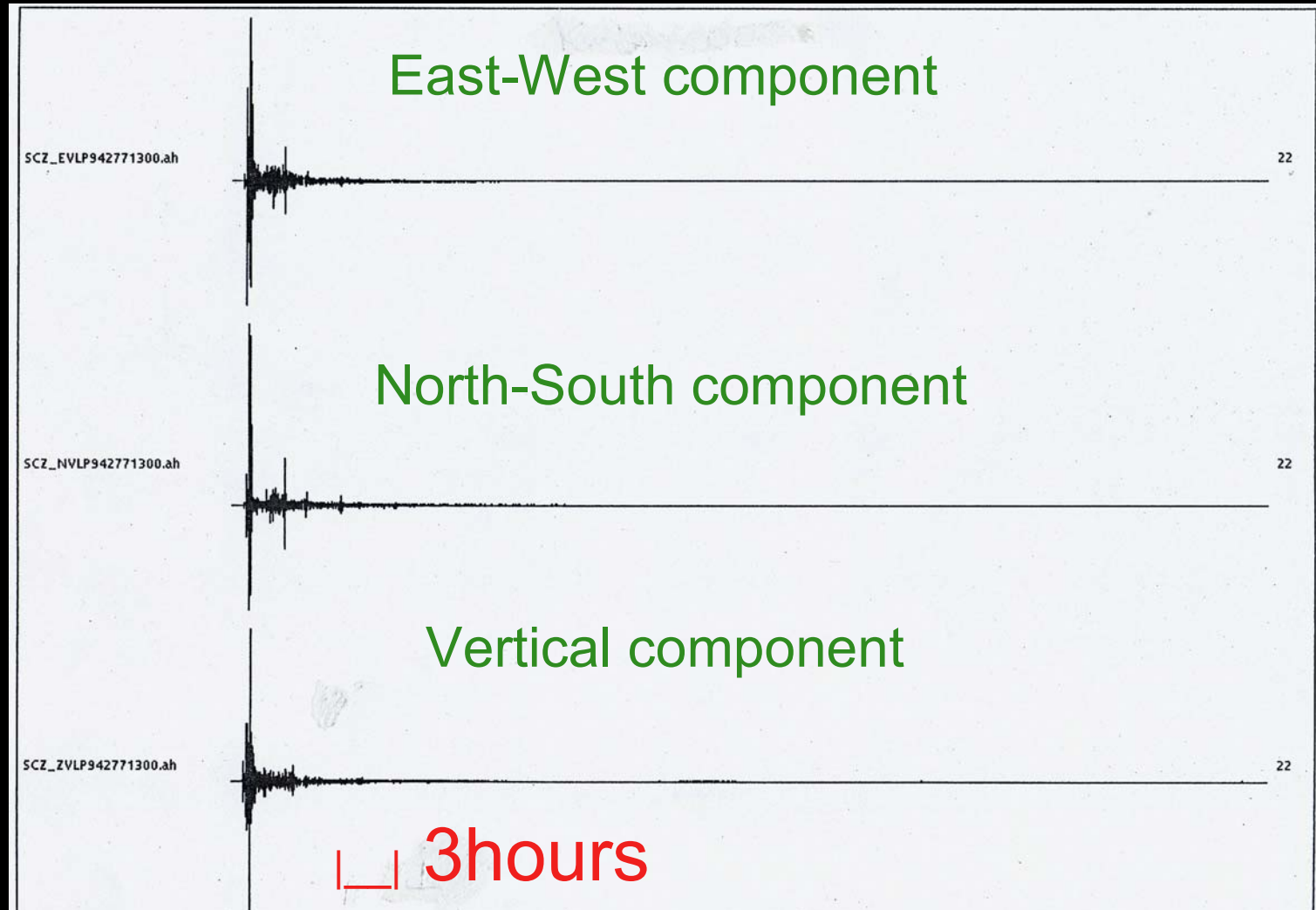
FIG. 3. — Spectre de l'enregistrement du pendule E (n° 1) — En haut : positions des pics théoriques pour les oscillations sphéroïdales S et les oscillations de torsion T du modèle de Gutenberg continental.

First observations of free oscillations of the Earth
1953? -> 1960 (Chile earthquake)

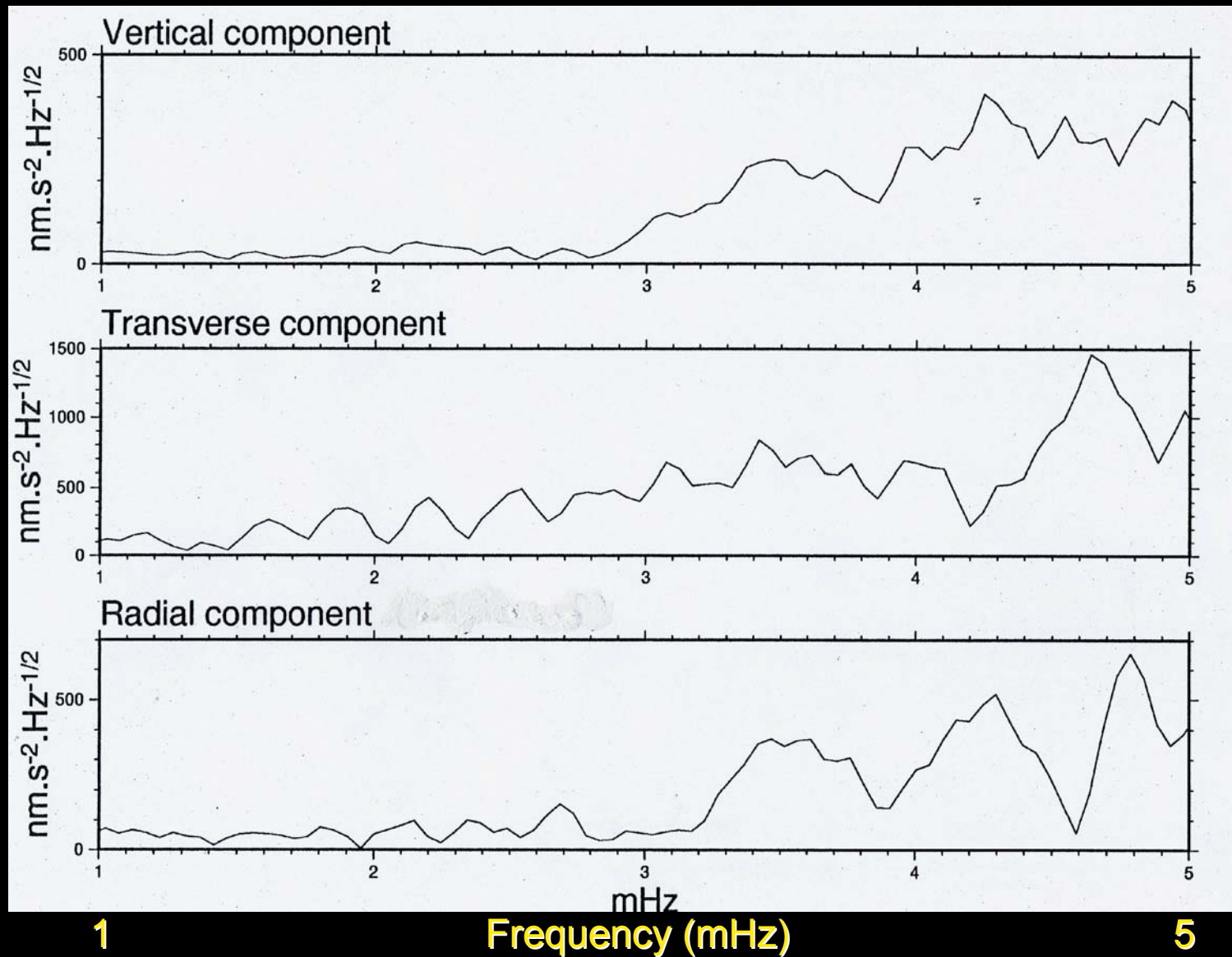
Frequency Peaks were not well understood

Theory was incomplete

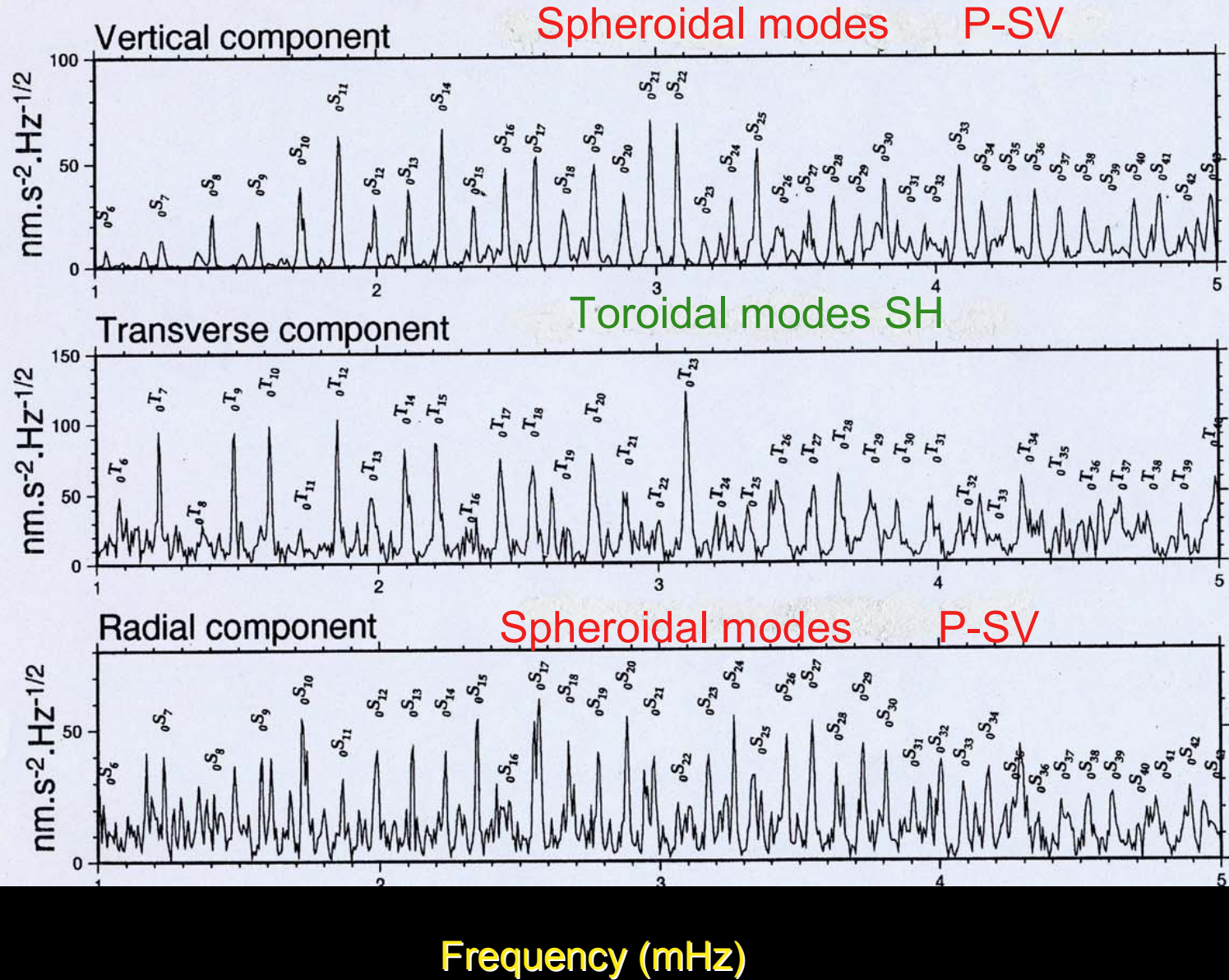
Kuril islands 1994-277 $M_s=8.3$



Kuril islands 1994-277 SCZ-VLP Spectra 3 hours



KURIL 94 277 - SCZ VLP - 36h.



Frequency (mHz)

Elastodynamic equation

$$\rho \partial_{tt} \mathbf{u}_{0i} = \partial_j \sigma_{ij} + \rho \mathbf{g}_i + \mathbf{F}_i (+ \mathbf{F} \mathbf{s}_i + \dots)$$

Which can be rewritten:

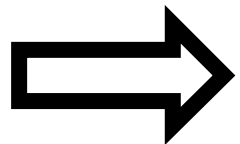
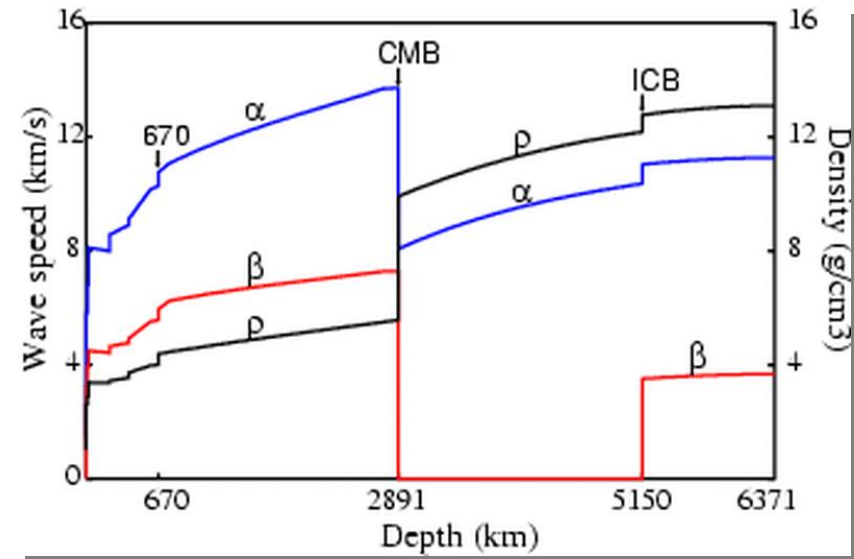
$$\rho \partial_{tt} \mathbf{u}_0 = \mathbf{H}_0 \mathbf{u}_0 (+ \mathbf{F} \mathbf{s})$$

\mathbf{H}_0 is an integro-differential operator

1D-Reference Earth Model:

$$M_0(r), \rho(r), V_P(r), V_S(r)$$

(PREM, Dziewonski and Anderson, 1981
or IASP91, Kennett and Engdahl, 1991)



John Woodhouse lecture

$$\rho \partial_{tt} \mathbf{u}_0 = \mathbf{H}_0 \mathbf{u}_0 \quad (+ \mathbf{F}s)$$

Eigenfrequencies: ${}_n \omega_l$

Eigenfunctions: ${}_n \mathbf{u}_l^m(\mathbf{r}, t) = |n, l, m\rangle \exp(-i {}_n \omega_l t)$

3 quantum numbers ($k = \{n, l, m\}$) $\Rightarrow \mathbf{u}_k(\mathbf{r}) \exp(-i {}_n \omega_l t)$

$$\int \rho \mathbf{u}_k^* \cdot \mathbf{u}_k d^3x = \delta_{ij}$$

$$\mathbf{H}_0 \mathbf{u}_k = \rho {}_n \omega_l^2 \mathbf{u}_k$$

Displacement:

$$\mathbf{u}(\mathbf{r}, t) = \sum_{n, l, m} {}_n \mathbf{a}_l^m |n, l, m\rangle \exp(-i {}_n \omega_l t)$$

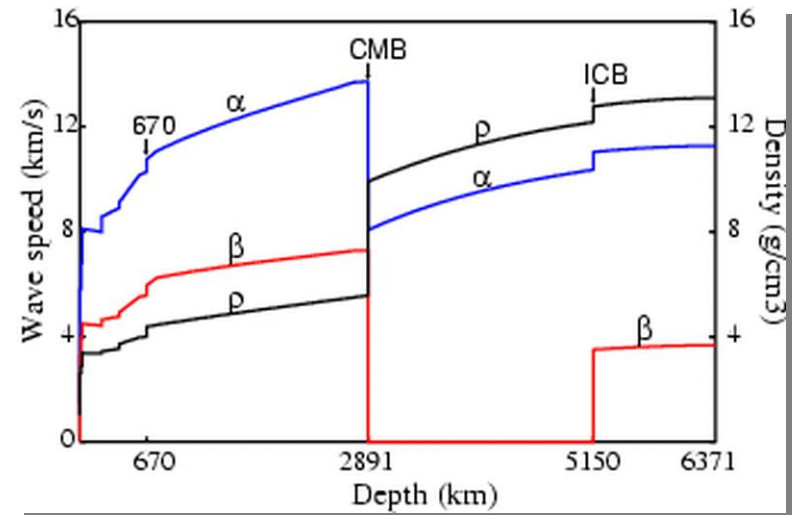
$$\begin{aligned} \mathbf{u}_k(\mathbf{r}) = & \{U(r)\mathbf{e}_r + V(r)\mathbf{e}_\theta \partial_\theta + V(r)/\sin\theta \mathbf{e}_\phi \partial_\phi\} Y_l^m(\theta, \phi) \\ & + \{W(r)/\sin\theta \mathbf{e}_\theta \partial_\phi - W(r) \mathbf{e}_\phi \partial_\theta\} Y_l^m(\theta, \phi) \end{aligned}$$

1D-Reference Earth Model:

$$M_0(r), \rho(r), V_P(r), V_S(r)$$

(PREM, Dziewonski and Anderson, 1981)

$$\rho \partial_{tt} \mathbf{u}_0 + \mathbf{H}_0 \mathbf{u}_0 = \mathbf{0}$$



Eigenfrequencies: ${}_n \omega_l$

Eigenfunctions: ${}_n u_l^m (r,t) = |n,l,m\rangle \exp(-i {}_n \omega_l t)$

2 kinds of modes: Toroidal ${}_n T_l$, Spheroidal ${}_n S_l$

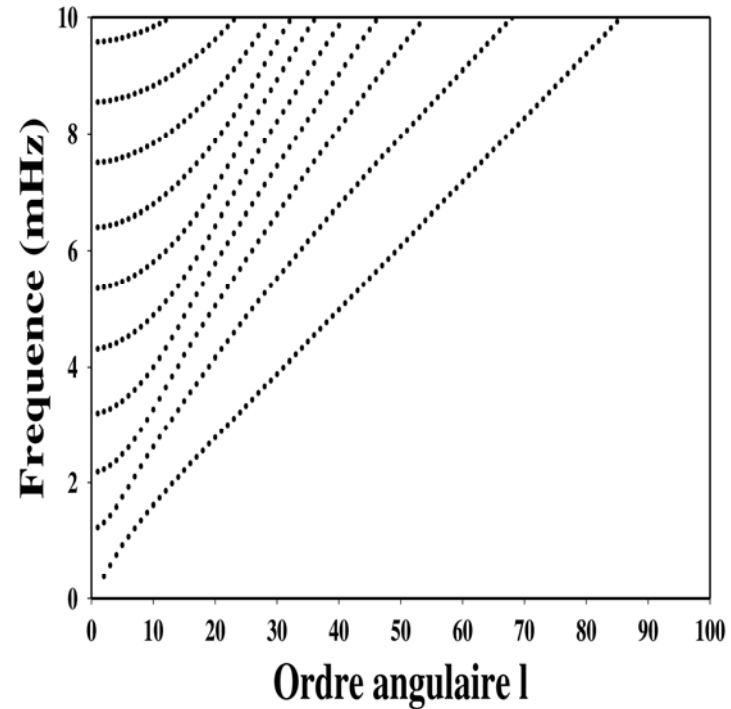
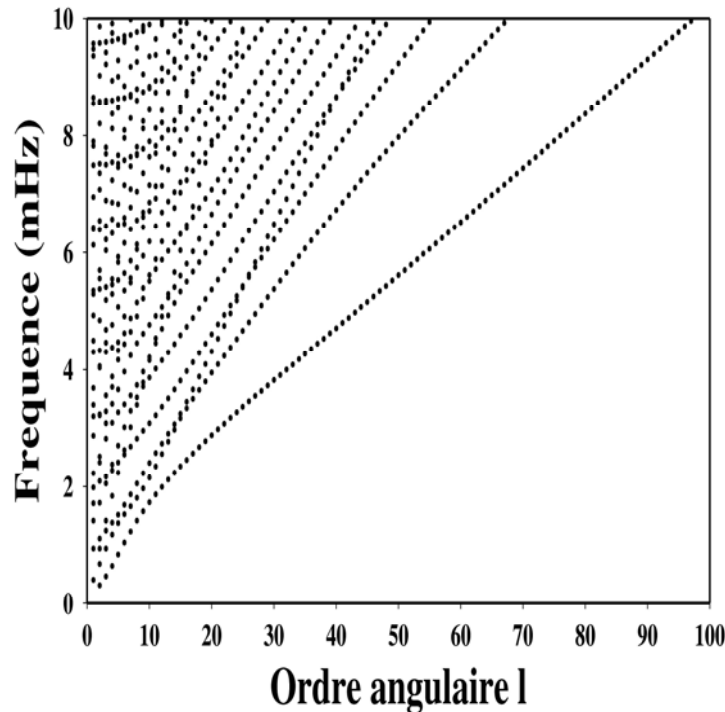
Degeneracy of eigenfrequencies ${}_n \omega_l : 2l + 1$

Spherical eigenfrequencies

Spheroidal Modes ${}_n S_l$
(P-SV / Rayleigh)

Toroidal modes ${}_n T_l$
(SH / Love)

Dispersion Branches



multiplet : $(n,l) = 2l+1$ singlets
singlet : (n,l,m)

n : radial order
 l : angular order
 m : azimuthal order

Spheroidal Modes

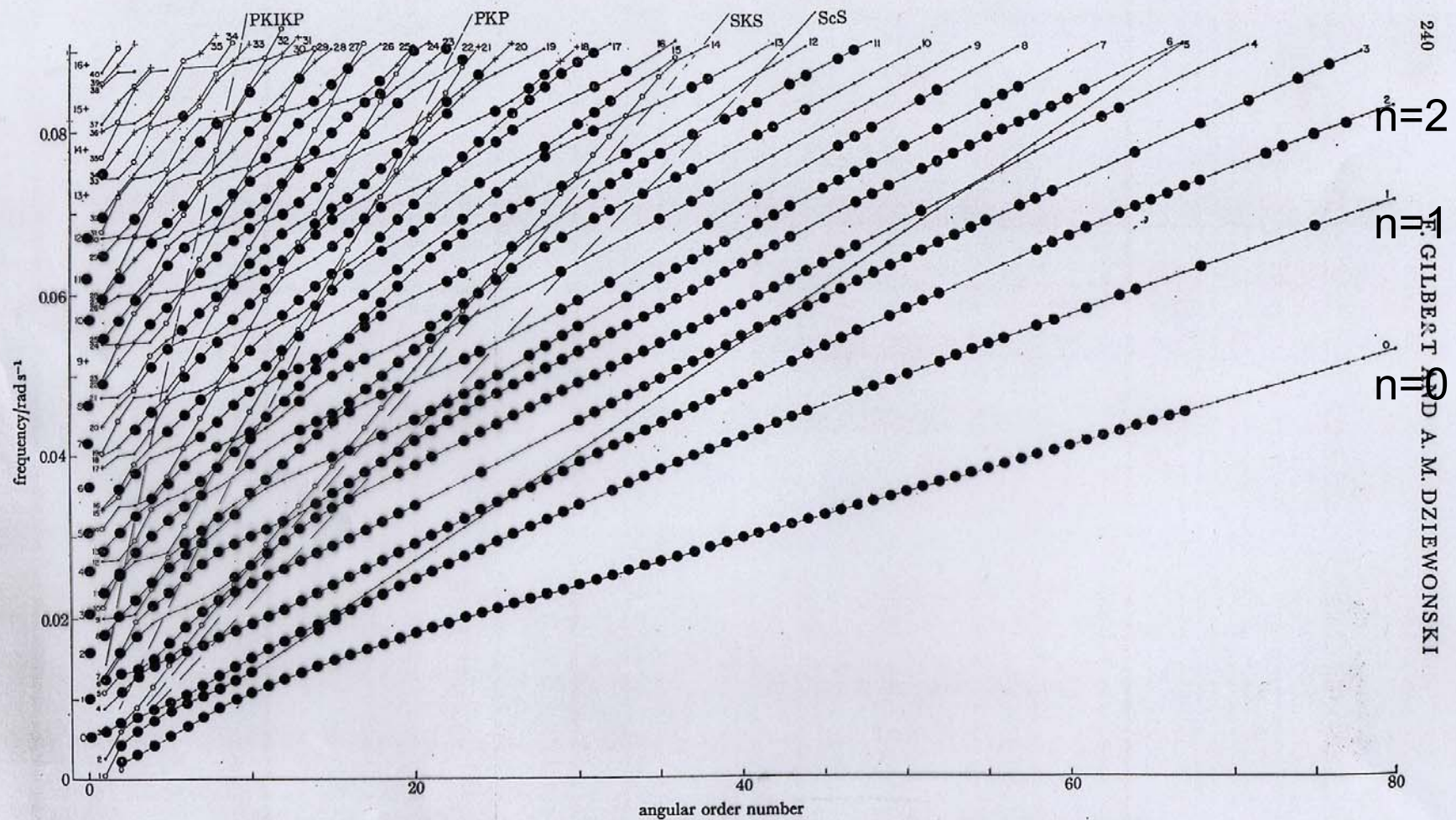
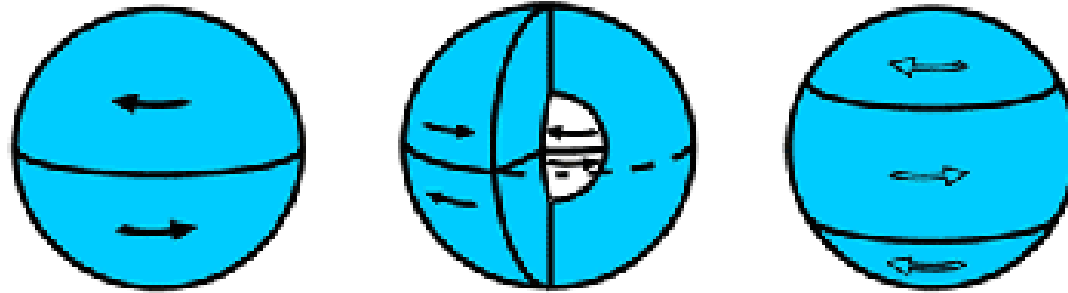
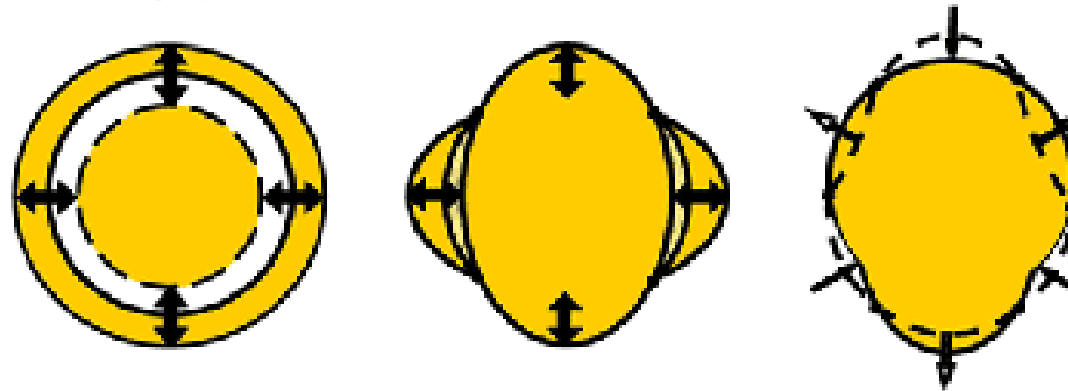


FIGURE 17. Spheroidal normal modes in the (ω, l) plane. The large dots indicate observed modes used in the inversions. For further details we refer the reader to §3 of Alaska II. •, $CE < 0.5$; +, $CE \geq 0.5$; o core modes.

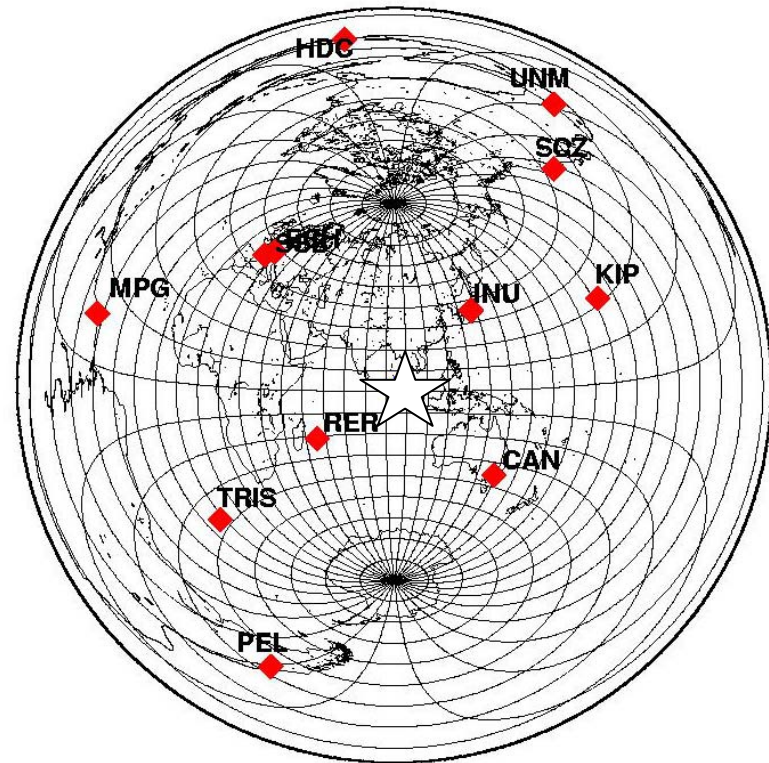
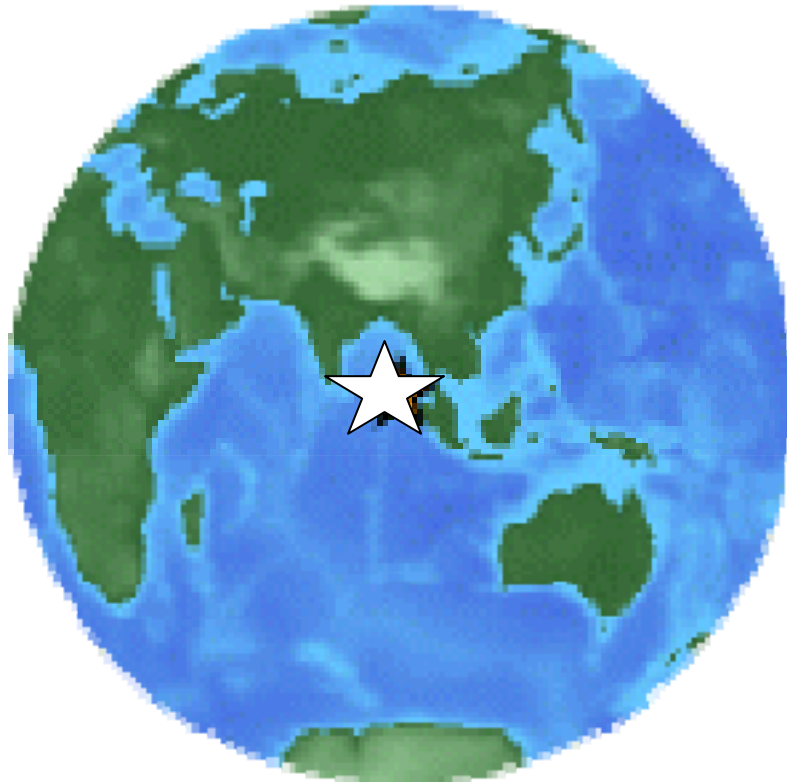


Toroidal modes ${}_0T_2$ (44.2 min), ${}_1T_2$ (12.6 min)
and ${}_0T_3$ (28.4 min)



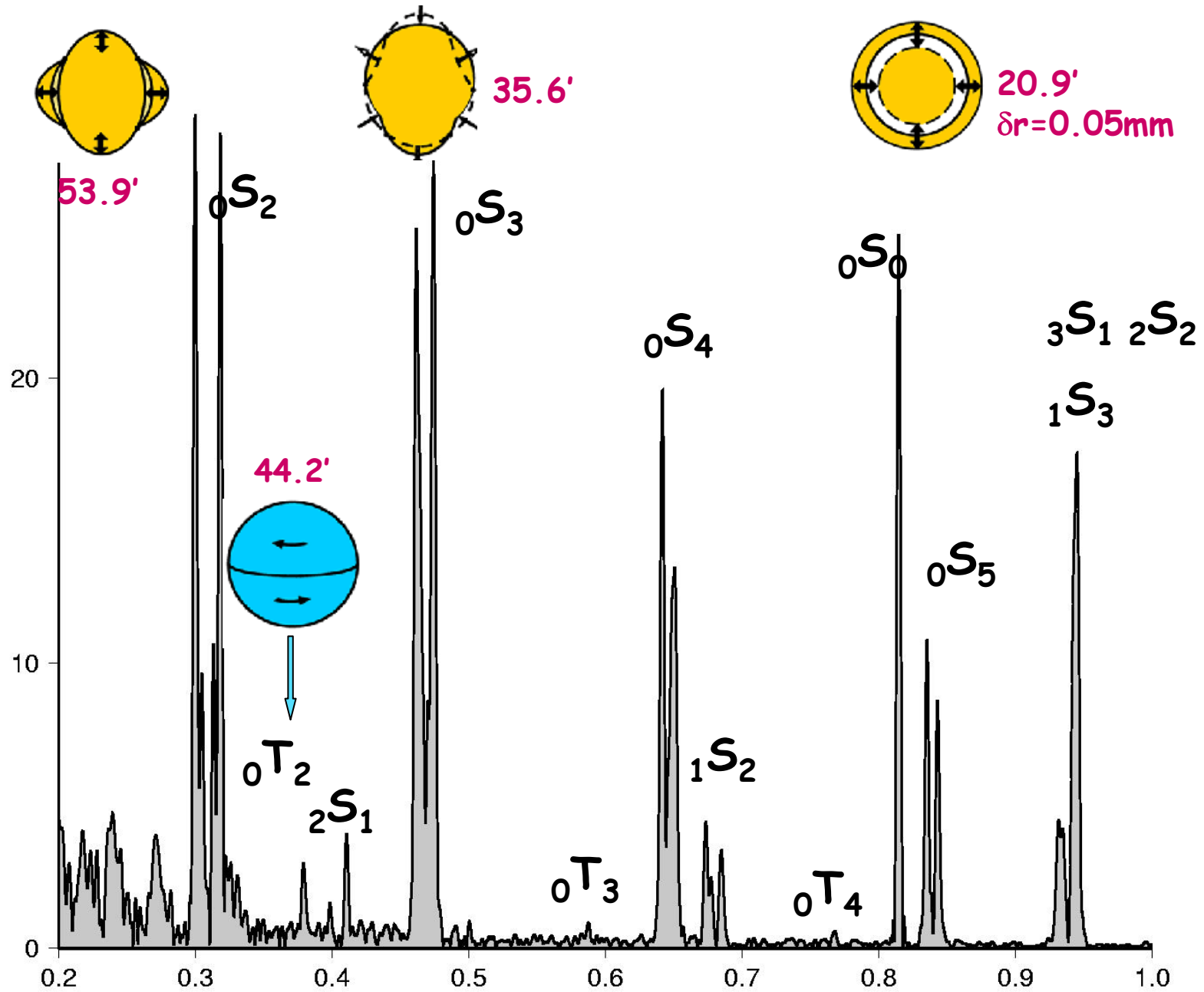
Spheroidal modes ${}_0S_0$ (20.5 min), ${}_0S_2$ (53.9 min)
and ${}_0S_3$ (35.6 min)

Study of Sumatra earthquake (26 december 2004) With GEOSCOPE stations



(Roult and Clévéde, 2005 ; Park et al., Science, 2005)

STS1
CAN

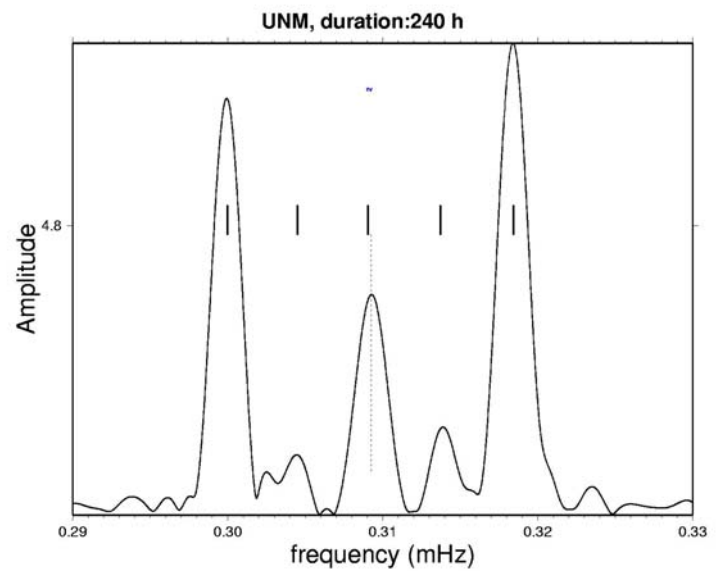
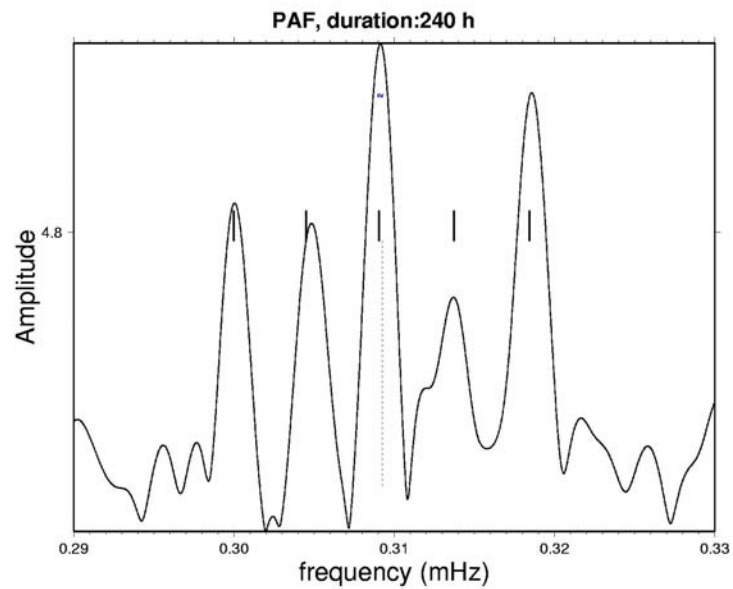
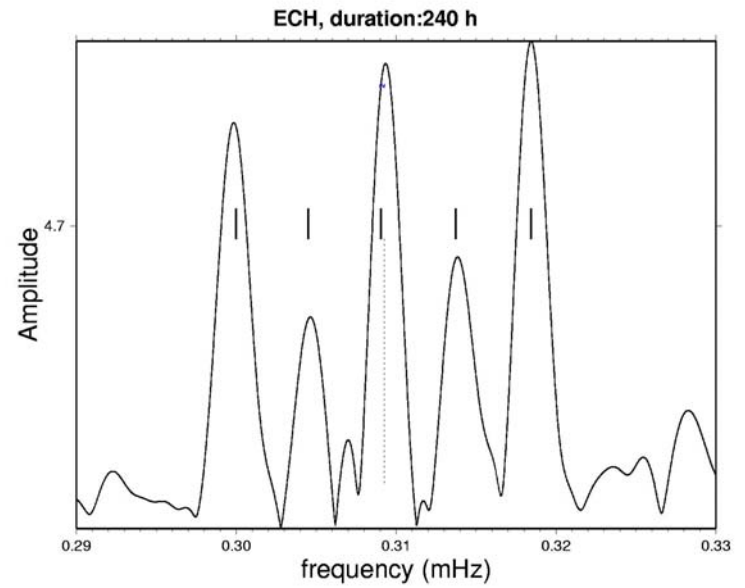
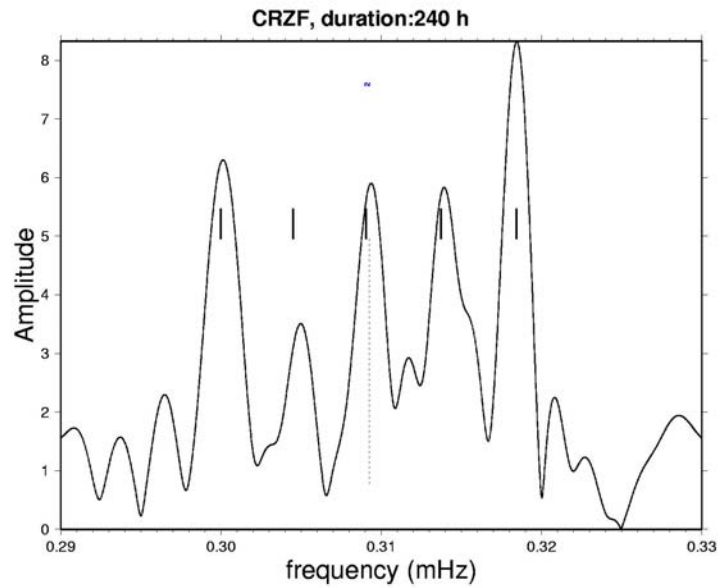


Sumatra-Andaman earthquake
26 December 2004

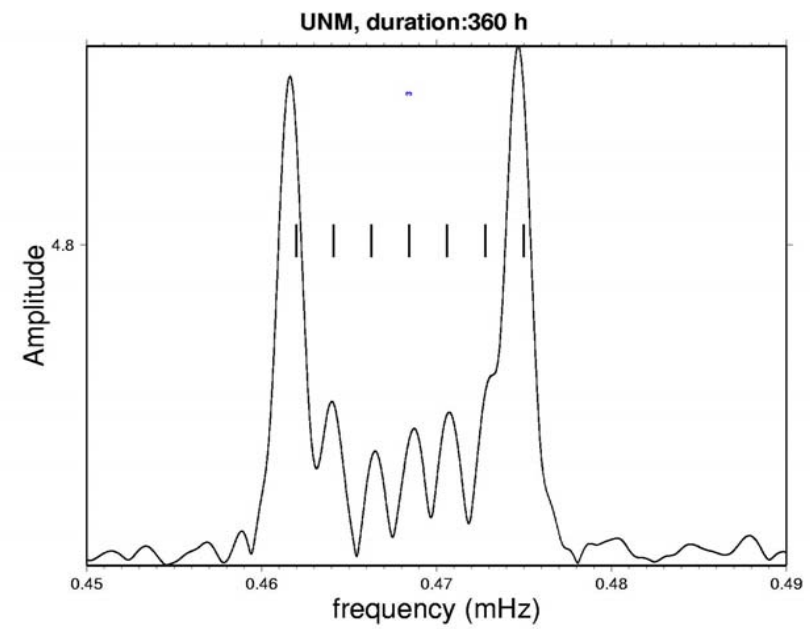
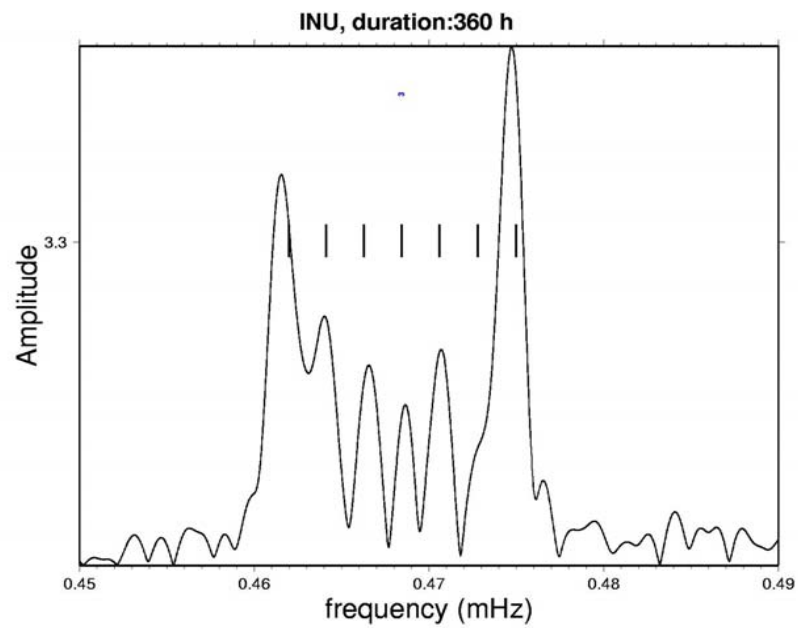
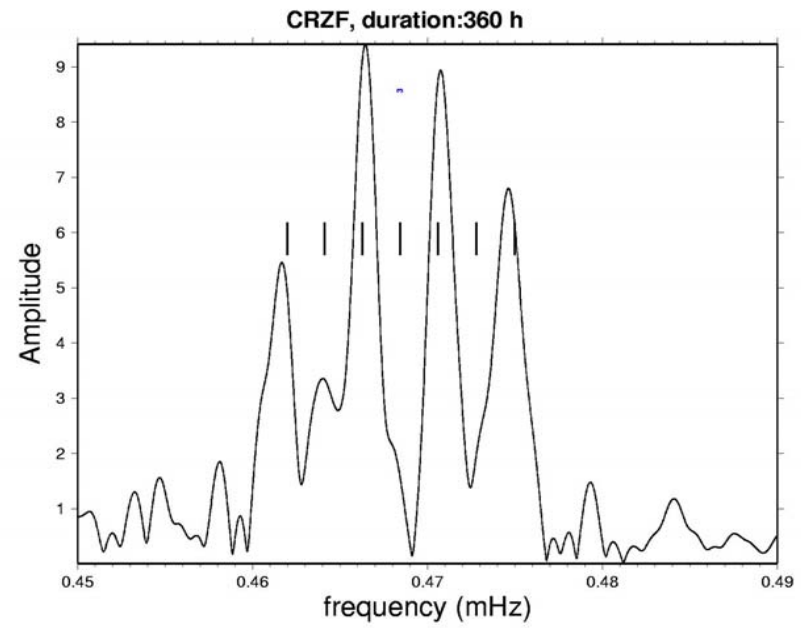
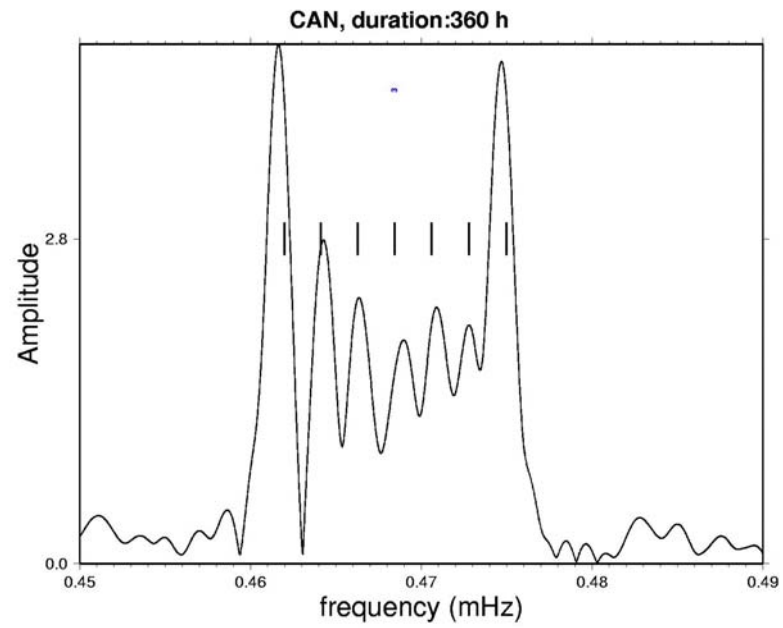
frequency (mHz)

Roult and Clévédé, 2005

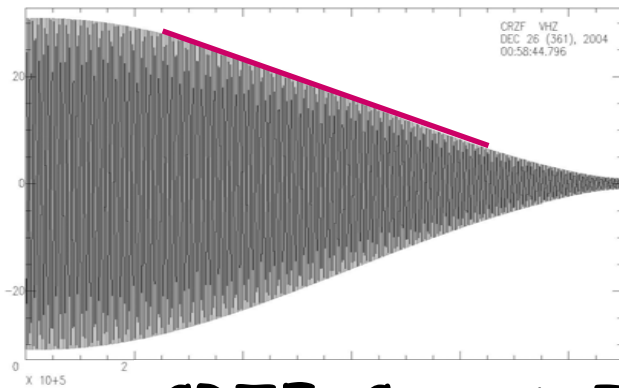
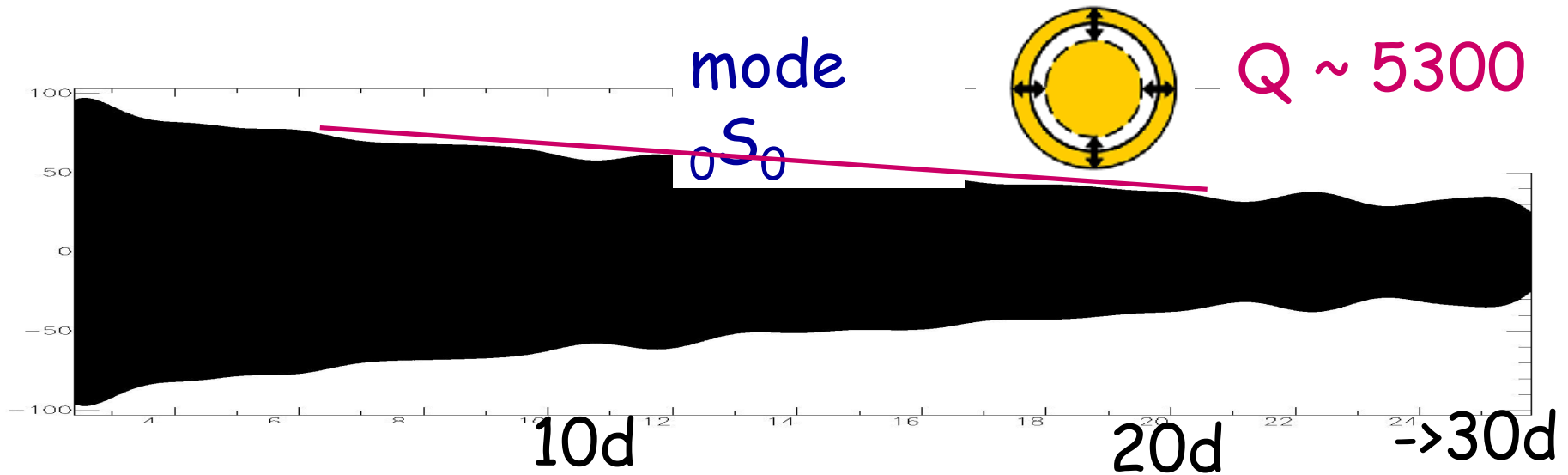
mode ${}_0S_2 \Rightarrow$ splitting 5 singlets



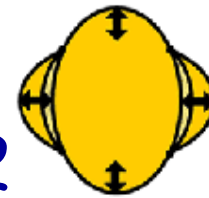
mode ${}_0S_3$



Attenuation of some modes



mode $0S_2$
singlet $m=+2$



$Q \sim 500$

CRZF, Crozet, Indian Ocean

Seismic Source

$$\rho \partial_{tt} \mathbf{u} + \mathbf{H}_0 \mathbf{u} = \mathbf{F}_s$$

Displacement at point \mathbf{r} and time t due to a force system \mathbf{F}_s at point source \mathbf{r}_s

eigenfrequencies: ω_l

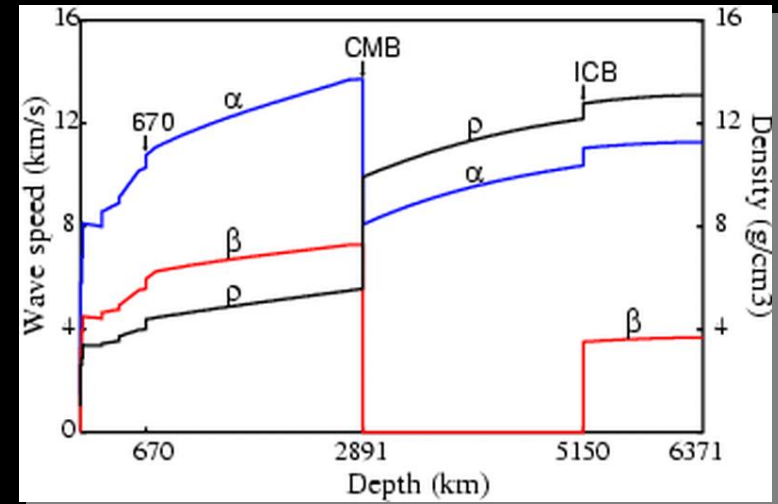
eigenfunctions: $\mathbf{u}_l^m(\mathbf{r}, t) = |n, l, m\rangle \exp(-i \omega_l t)$

$$\mathbf{u}(\mathbf{r}, t) = \sum_{n, l, m} \mathbf{a}_l^m |n, l, m\rangle \exp(-i \omega_l t)$$

Eigenfunction basis is a complete basis \Rightarrow any wave can be modelled by normal mode summation including surface waves and body waves.

1D- Reference Earth Model

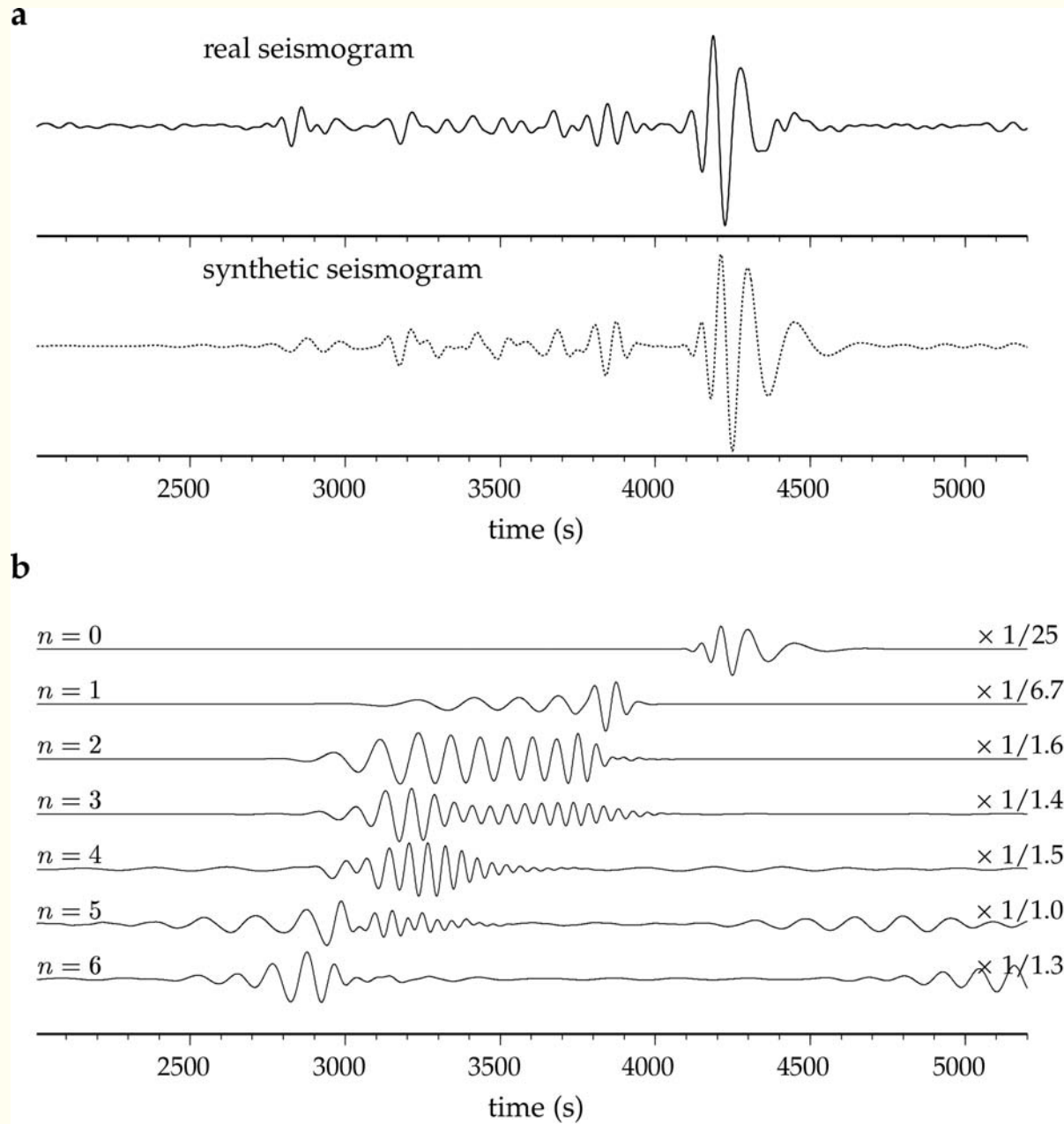
Synthetic Seismograms
by normal mode
summation $\mathbf{u}_k(k=\{n,l,m\})$.



$$\mathbf{u}(\mathbf{r},t) = \sum_k \mathbf{u}_k(\mathbf{r}) \cos \omega_k t / \omega_k^2 \exp(-\omega_k t / 2Q_k) (\mathbf{u}_k \cdot \mathbf{F})_S$$

$$\text{Source Term } (\mathbf{u}_k \cdot \mathbf{F})_S = (\mathbf{M} : \boldsymbol{\varepsilon})_S$$

\mathbf{M} Seismic moment tensor, $\boldsymbol{\varepsilon}$ deformation tensor



Beucler et al., 2003

Data

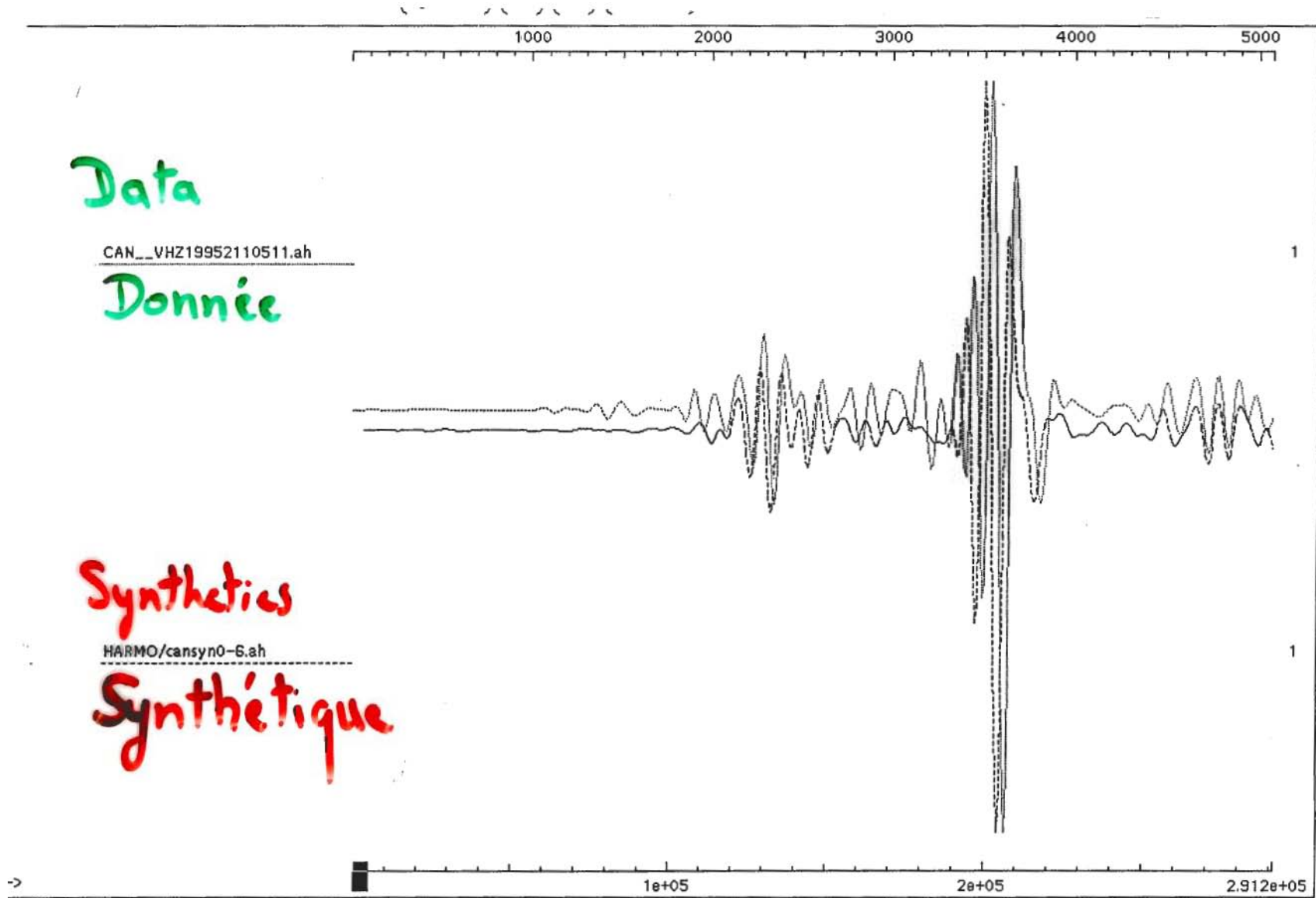
CAN_VHZ19952110511.ah

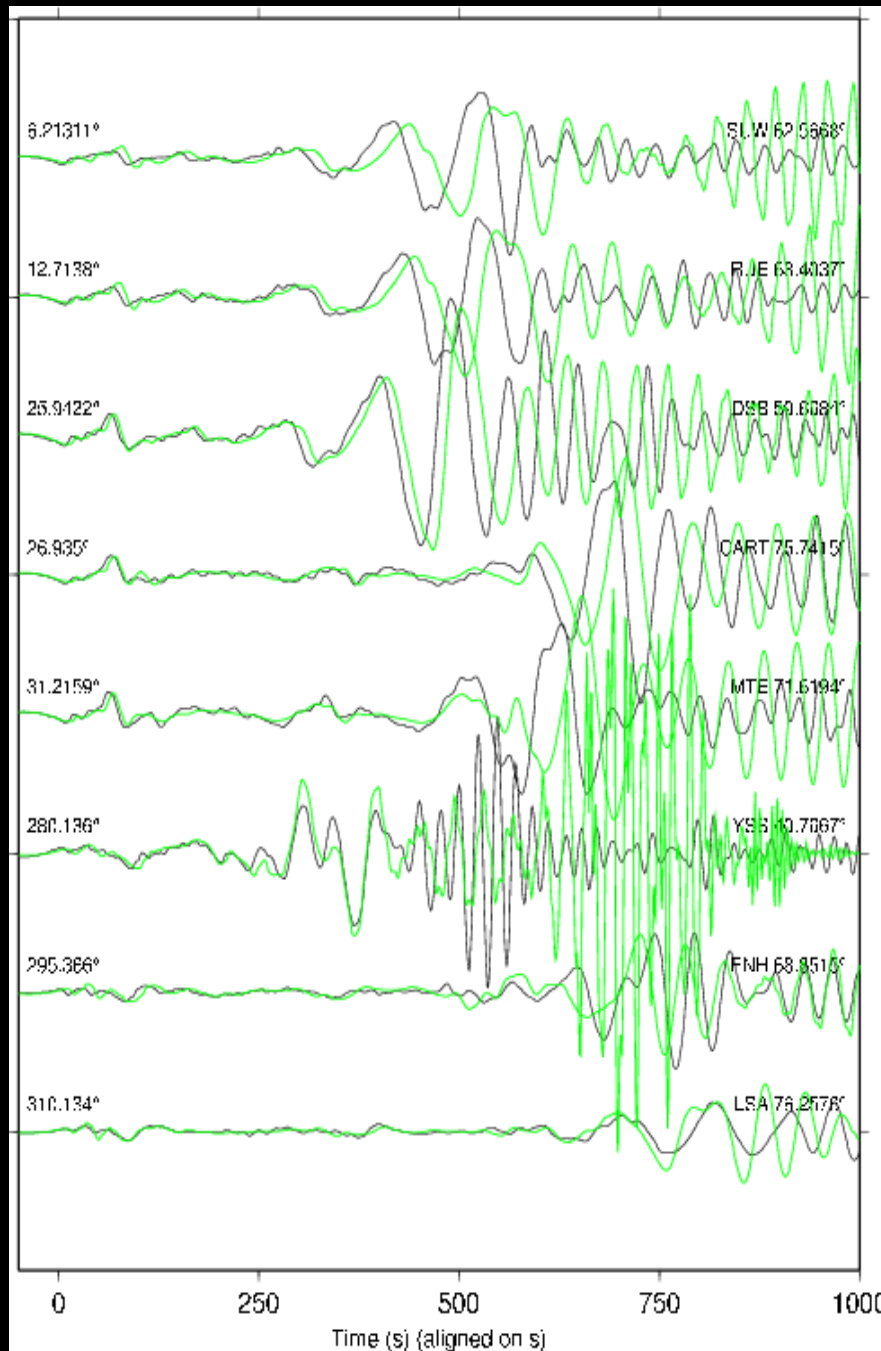
Donnée

Synthetics

HARMO/cansyn0-6.ah

Synthétique





**Synthetic seismograms
By normal mode
summation**

**Denali-Alaska
earthquake (Nov. 2002)**

Komatitsch and Tromp, 2003

Duality wave - particle:

λ seismic wavelength

Λ scale heterogeneity

Particle: **Ray** theory $\lambda \ll \Lambda$

=> Finite frequency effects (**Guust Nolet**)

Wave: Normal **Mode** theory (NM) + Perturbation theories (small amplitude of 3D- heterogeneities) =>
(**John Woodhouse**)

Numerical modelling of wave equation

Strong or weak forms: $\lambda \approx \Lambda$

-Spectral Element Method (SEM)



(**Dimitri Komatitsch**)

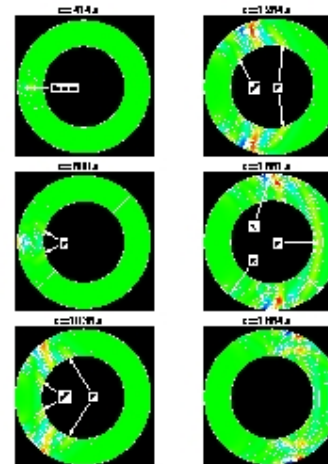
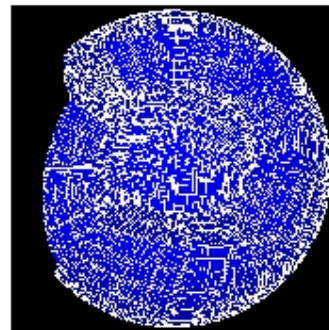
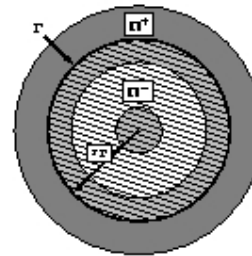
-Coupled SEM-NM method

Spectral Element Method: D. Komatitsch (1999)

Coupled method of Spectral Elements and Modal Solution

Principle:

- Ω^+ : Spectral Element area:
3D model
- Ω^- : Modal Solution area:
1D model



Capdeville et al., 2002

Overview

Large scale Seismology: an observational field

- Data (Seismic source) + Instrument (Seismometer)
-> Observations (seismograms)
- Historical evolution: Ray theory, Normal mode theory, Numerical techniques (SEM, NM-SEM)
- **Scientific Issues: Earthquakes (Sumatra), Anisotropic structure of the Earth**
- Tomographic Technique
- Geodynamic Applications.
Seismic Experiment Plume detection
- NM-SEM and time reversal

Seismic Source Studies

$$\mathbf{u}(\mathbf{r},t) = \sum_k S_k u_k(\mathbf{r}) \cos \omega_k t / \omega_k^2 \exp(-\omega_k t / 2Q) (\mathbf{u}_k \cdot \mathbf{F})_S$$

Source Term $(\mathbf{u}_k \cdot \mathbf{F})_S = (\mathbf{M} : \boldsymbol{\varepsilon})_S$

M Seismic moment tensor, $\boldsymbol{\varepsilon}$ deformation tensor

